

Article

Synthesis of New Triazole-Based Thiosemicarbazone Derivatives as Anti-Alzheimer's Disease Candidates: Evidence-Based In Vitro Study

Fazal Rahim ^{1,*}, Hayat Ullah ^{2,*}, Muhammad Taha ³, Rifaqat Hussain ¹, Maliha Sarfraz ⁴, Rashid Iqbal ⁵, Naveed Iqbal ⁶, Shoaib Khan ¹, Syed Adnan Ali Shah ^{7,8}, Marzough Aziz Albalawi ⁹, Mahmoud A. Abdelaziz ¹⁰, Fatema Suliman Alatawi ¹¹, Abdulrahman Alasmari ¹², Mohamed I. Sakran ^{11,13}, Nahla Zidan ^{14,15}, Ibrahim Jafri ¹⁶ and Khalid Mohammed Khan ¹⁷

¹ Department of Chemistry, Hazara University, Mansehra 21120, Pakistan

² Department of Chemistry, University of Okara, Okara 56130, Pakistan

³ Department of Clinical Pharmacy, Institute for Research and Medical Consultations (IRMC), Imam Abdulrahman Bin Faisal University, Dammam 31441, Saudi Arabia

⁴ Department of Zoology, Wildlife and Fisheries, Sub-Campus Toba Tek Singh, University of Agriculture Faisalabad, Punjab 36050, Pakistan

⁵ Department of Agronomy, Faculty of Agriculture and Environment, The Islamia University of Bahawalpur, Bahawalpur 63100, Pakistan

⁶ Department of Chemistry, University of Poonch, Rawalakot 12350, Pakistan

⁷ Faculty of Pharmacy, Universiti Teknologi MARA Cawangan Selangor Kampus Puncak Alam, Bandar Puncak Alam 42300, Selangor, Malaysia

⁸ Atta-ur-Rahman Institute for Natural Product Discovery (AuRIns), Universiti Teknologi MARA Cawangan Selangor Kampus Puncak Alam, Bandar Puncak Alam 42300, Selangor, Malaysia

⁹ Department of Chemistry, Alwajh College, University of Tabuk, Tabuk 47512, Saudi Arabia

¹⁰ Department of Chemistry, Faculty of Science, University of Tabuk, Tabuk 71491, Saudi Arabia

¹¹ Department of Biochemistry, Faculty of Science, University of Tabuk, Tabuk 71491, Saudi Arabia

¹² Department of Biology, Faculty of Science, University of Tabuk, Tabuk 71491, Saudi Arabia

¹³ Biochemistry Section, Chemistry Department, Faculty of Science, Tanta University, Tanta 31527, Egypt

¹⁴ Department of Nutrition and Food Science, Faculty of Home Economics, University of Tabuk, Tabuk 71491, Saudi Arabia

¹⁵ Department of Home Economics, Faculty of Specific Education, Kafr ElSheikh University, Kafr ElSheikh 33516, Egypt

¹⁶ Department of Biotechnology, Faculty of Sciences, Taif University, Taif 21944, Saudi Arabia

¹⁷ H.E.J. Research Institute of Chemistry, International Center for Chemical and Biological Sciences, University of Karachi, Karachi 75270, Pakistan

* Correspondence: fazalstar@gmail.com (F.R.); ayaanwazir366@gmail.com (H.U.)



Citation: Rahim, F.; Ullah, H.; Taha, M.; Hussain, R.; Sarfraz, M.; Iqbal, R.; Iqbal, N.; Khan, S.; Ali Shah, S.A.; Albalawi, M.A.; et al. Synthesis of New Triazole-Based Thiosemicarbazone Derivatives as Anti-Alzheimer's Disease Candidates: Evidence-Based In Vitro Study. *Molecules* **2023**, *28*, 21. <https://doi.org/10.3390/molecules28010021>

Academic Editor: Antonio Palumbo Piccionelli

Received: 18 October 2022

Revised: 27 November 2022

Accepted: 8 December 2022

Published: 20 December 2022



Copyright: © 2022 by the authors. Licensee MDPI, Basel, Switzerland. This article is an open access article distributed under the terms and conditions of the Creative Commons Attribution (CC BY) license (<https://creativecommons.org/licenses/by/4.0/>).

Abstract: Triazole-based thiosemicarbazone derivatives (**6a–u**) were synthesized then characterized by spectroscopic techniques, such as ¹HNMR and ¹³CNMR and HRMS (ESI). Newly synthesized derivatives were screened in vitro for inhibitory activity against acetylcholinesterase (AChE) and butyrylcholinesterase (BuChE) enzymes. All derivatives (except **6c** and **6d**, which were found to be completely inactive) demonstrated moderate to good inhibitory effects ranging from 0.10 ± 0.050 to 12.20 ± 0.30 μM (for AChE) and 0.20 ± 0.10 to 14.10 ± 0.40 μM (for BuChE). The analogue **6i** (IC₅₀ = 0.10 ± 0.050 for AChE and IC₅₀ = 0.20 ± 0.050 μM for BuChE), which had di-substitutions (2-nitro, 3-hydroxy groups) at ring B and tri-substitutions (2-nitro, 4,5-dichloro groups) at ring C, and analogue **6b** (IC₅₀ = 0.20 ± 0.10 μM for AChE and IC₅₀ = 0.30 ± 0.10 μM for BuChE), which had di-Cl at 4,5, -NO₂ groups at 2-position of phenyl ring B and hydroxy group at ortho-position of phenyl ring C, emerged as the most potent inhibitors of both targeted enzymes (AChE and BuChE) among the current series. A structure-activity relationship (SAR) was developed based on nature, position, number, electron donating/withdrawing effects of substitution/s on phenyl rings. Molecular docking studies were used to describe binding interactions of the most active inhibitors with active sites of AChE and BuChE.

Keywords: triazole; thiosemicarbazone; acetylcholinesterase; butyrylcholinesterase; structure activity relationship; molecular docking study

1. Introduction

Alzheimer's disease (AD) is an irreversible, neurodegenerative and progressive disorder of the brain that diminishes the cholinergic system and results in disorientation, memory loss, impaired ability to solve problems and impaired cognition [1–3]. AD is the major cause of dementia in aging populations. The acetylcholinesterase (AChE) and butyrylcholinesterase (BuChE) enzymes cause apoptosis of neuronal cells by plaques formed by aggregation of neurotoxic beta amyloid. They are involved in hydrolysis of acetylcholine to generate acetic acid and choline, leading to shortening of duration of acetylcholine in the hippocampus and cortex of the brain and thus facilitating normal regeneration of synapses and functioning. Therefore, targeting both AChE and BuChE enzymes is one approach for treatment of AD [4–7]. Two binding sites are present in AChE: the peripheral site, which is responsible for beta amyloid interaction, and the catalytic site, which causes hydrolysis of acetylcholine. Interactions of beta amyloid protein ($A\beta$) with AChE access the formation of beta amyloid protein-acetylcholinesterase ($A\beta$ -AChE) complex and thus result in neurotoxicity. BuChE is found in liver, intestine, heart, kidney, serum and lungs, while AChE is present in cholinergic neurons, brain and muscle [8,9]. The cholinesterase enzymes perform key roles in the breakdown of compounds, having ester moieties in their core structures. Generally, AChE is dominant in brain, while BuChE functions when acetylcholine gradually decreases its function in the brain of AD patients. Hence, synthesis of drugs that function as inhibitors of both AChE and BuChE enzymes should be effective treatments of AD [10]. Several drugs have been approved by the Food and Drug Administration (FDA) for treatment of AD. These include galantamine and donepezil which are selective for AChE, while rivastigmine and tacrine inhibit both BuChE and AChE (Figure 1) [11].

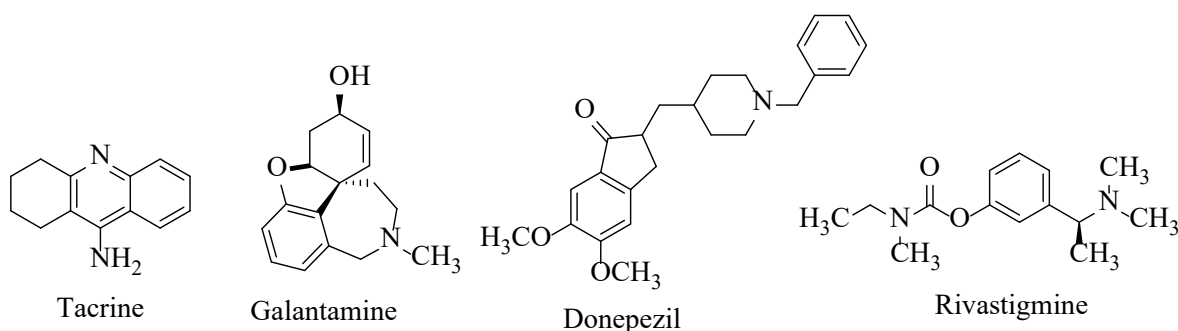


Figure 1. Available drugs for Alzheimer's disease.

Triazole analogues are reported to have therapeutic and biological activities, such as anticonvulsant [12], anti-inflammatory [13], antifungal [14], insecticidal [15] and plant growth regulation [16]. There are some important drugs, such as letrozole (anticancer), tazobactam (antibacterial), isavuconazole (antifungal), sitagliptin (antidiabetic), ribavirin (antiviral), and rufinamide (seizure disorder), that contain triazole moieties in their core structures (Figure 2) [17–23].

Recently, several classes of heterocyclic compounds have been reported to be potent inhibitors of acetylcholinesterase (AChE) and butyrylcholinesterase (BuChE) [24–28]. Based on the biological importance of thiosemicarbazone [29,30] and triazole [31,32] compounds (Figure 3), it was decided to synthesize hybrid analogues based on triazole bearing thiosemicarbazone moiety as effective inhibitors of cholinesterase enzymes, such as AChE and BuChE, that could be effective treatments for AD.

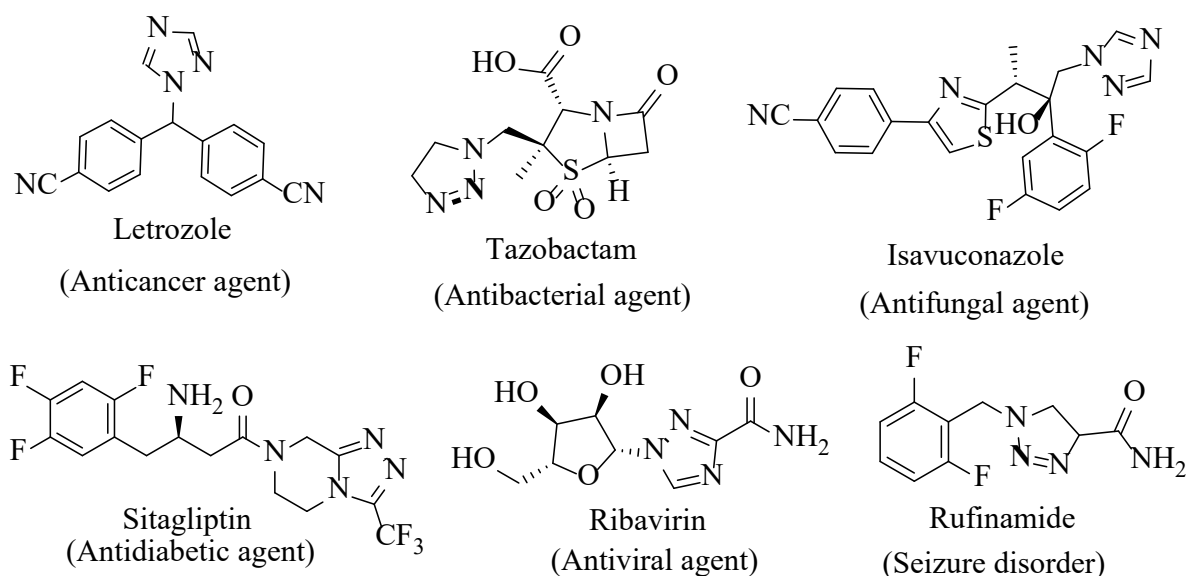


Figure 2. Bioactive drugs with triazole moiety.

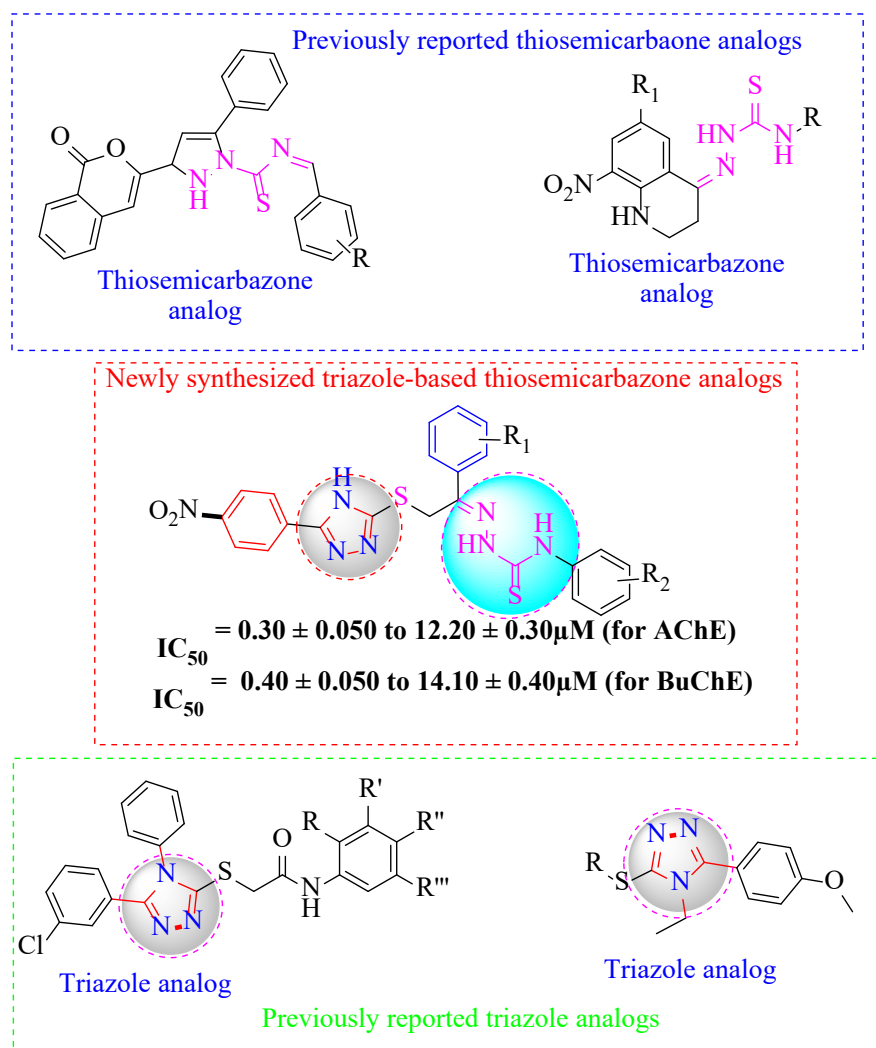
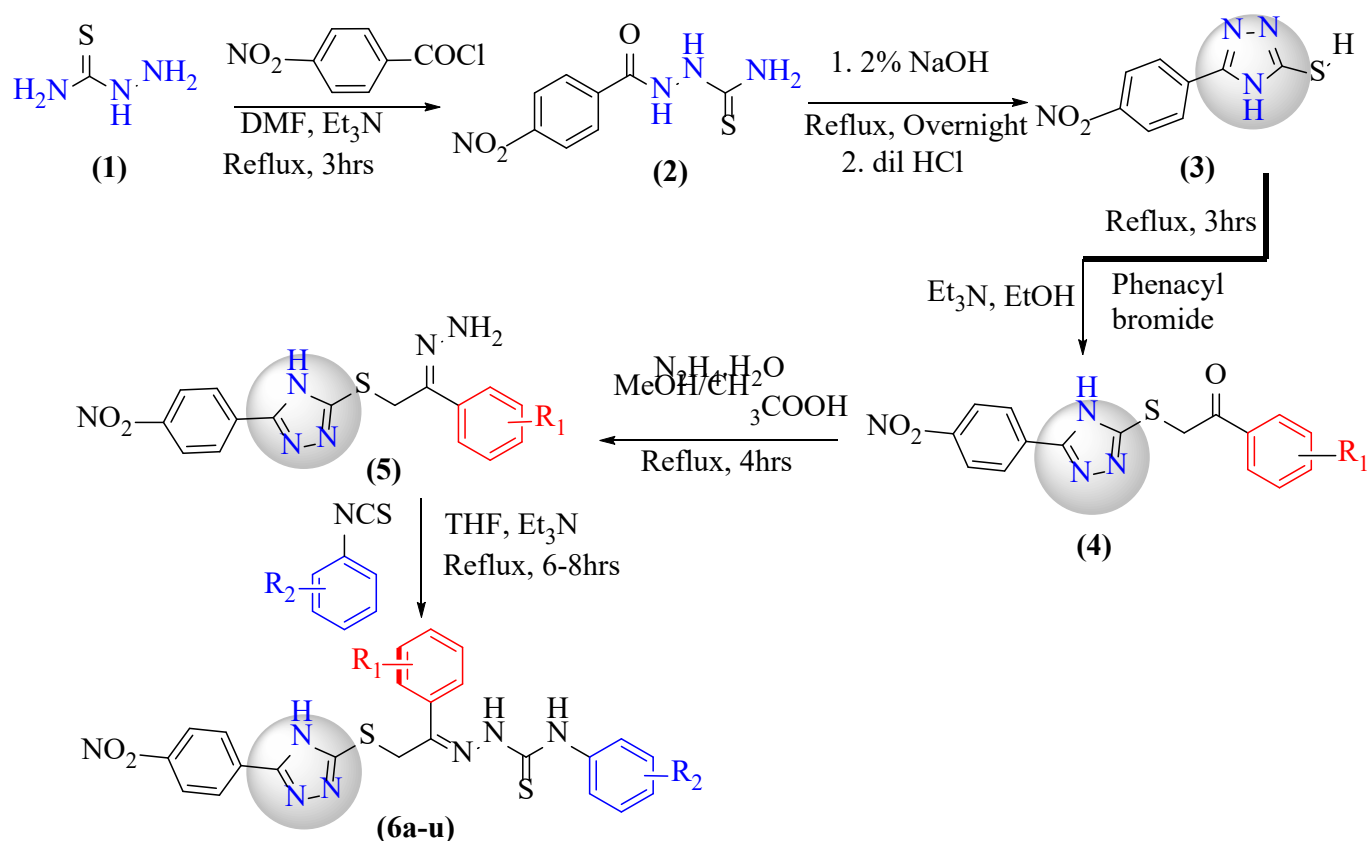


Figure 3. Rationale of the current study.

2. Results and Discussion

2.1. Chemistry

Thiosemicarbazide (1) was treated with 4-nitrobenzoyl chloride in DMF in the presence of triethylamine and refluxed for 3 h to yield 2-(4-nitrobenzoyl)hydrazine-1-carbothioamide as the first intermediate (2), which further underwent cyclization during stirring overnight in 2% aqueous solution of sodium hydroxide followed by neutralization with dil. HCl to yield 1,2,4-triazole-3-thiole (3) as the second intermediate product. Intermediate (3) was then reacted with different substituted phenacyl bromide in ethanol in the presence of triethylamine and refluxed for 3 h to obtain the third intermediate (4). Intermediate (4) was then mixed with hydrazine hydrate in methanol in the presence of a few drops of glacial acetic acid to form intermediate (5). Finally, intermediate (5) was treated with different substituted isothiocyanate in tetrahydrofuran in the presence of triethylamine, with the resulting mixture stirred under reflux until conversion had been completed, as monitored by TLC during refluxing for 6–8 h. After being cooled to room temperature, the product was reacted with 5% Na₂S₂O₃ and extracted with CH₂Cl₂/MeOH (10:1, 10 mL × 4). The combined organic layer was dried over anhydrous sodium sulfite and concentrated. The resulting residue was purified through silica gel column chromatography using a mixture of petroleum ether and EtOAc as eluent to yield the desired triazole-based thiosemicarbazone derivatives (6a–u) as the final product (Scheme 1, Table 1). Primary confirmation of the product was done using thin layer chromatography (TLC) and further confirmed by with nuclear magnetic resonance (NMR).



Scheme 1. Synthesis of triazole-based thiosemicarbazone derivatives (6a–u).

Table 1. Substituents, in vitro acetylcholinesterase and butyrylcholinesterase inhibitory activities, and selectivity index of triazole-based thiosemicarbazone derivatives (6a–u).

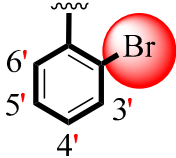
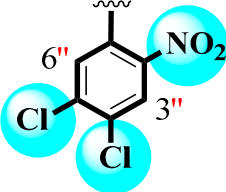
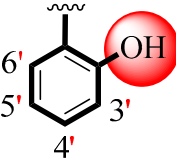
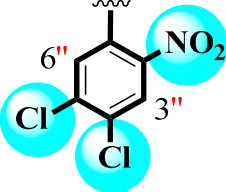
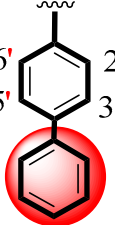
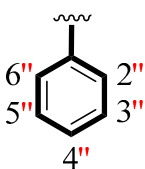
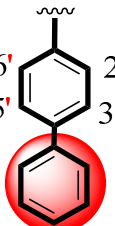
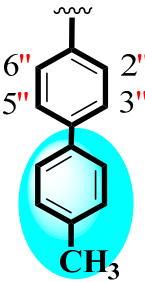
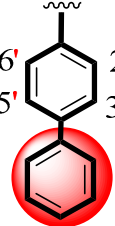
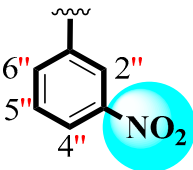
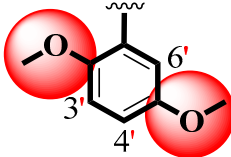
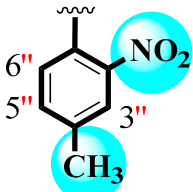
Derivative	R ₁	R ₂	AChE IC ₅₀ (μM) ^a	BuChE IC ₅₀ (μM) ^a	Selectivity Index ^b
6a			2.20 ± 0.10	3.90 ± 0.10	1.77
6b			0.20 ± 0.10	0.30 ± 0.10	1.5
6c			N.A.	N.A.	N.A.
6d			N.A.	N.A.	N.A.
6e			4.70 ± 0.10	6.30 ± 0.10	1.34
6f			2.40 ± 0.10	4.70 ± 0.10	1.96

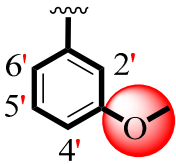
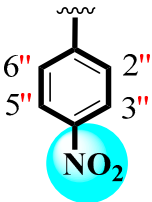
Table 1. Cont.

Derivative	R ₁	R ₂	AChE IC ₅₀ (μM) ^a	BuChE IC ₅₀ (μM) ^a	Selectivity Index ^b
6g			2.10 ± 0.10	4.30 ± 0.10	2.04
6h			9.10 ± 0.20	11.20 ± 0.30	1.23
6i			0.10 ± 0.050	0.20 ± 0.050	2.0
6j			11.30 ± 0.30	12.30 ± 0.30	1.09
6k			12.20 ± 0.30	14.10 ± 0.40	1.15
6l			4.60 ± 0.010	5.90 ± 0.10	1.28
6m			2.70 ± 0.10	3.80 ± 0.10	1.41

Table 1. Cont.

Derivative	R ₁	R ₂	AChE IC ₅₀ (μM) ^a	BuChE IC ₅₀ (μM) ^a	Selectivity Index ^b
6n			0.70 ± 0.05	1.70 ± 0.050	2.43
6o			2.50 ± 0.30	3.10 ± 0.40	1.24
6p			3.20 ± 0.10	4.60 ± 0.10	1.44
6q			0.60 ± 0.050	0.90 ± 0.10	1.50
6r			1.30 ± 0.050	2.20 ± 0.10	1.69
6s			1.40 ± 0.050	2.30 ± 0.10	1.64
6t			1.90 ± 0.10	2.50 ± 0.10	1.32

Table 1. Cont.

Derivative	R ₁	R ₂	AChE IC ₅₀ (μM) ^a	BuChE IC ₅₀ (μM) ^a	Selectivity Index ^b
6u			2.90 ± 0.10	3.70 ± 0.10	1.28
	Standard drug Donepezil		2.16 ± 0.12	4.5 ± 0.11	2.08

Note: ^a Values expressed as means ± standard error of three experiments. ^b Selectivity index: IC₅₀ of BuChE/IC₅₀ of AChE; N.A.: not active.

2.2. In Vitro Inhibition of Acetylcholinesterase and Butyrylcholinesterase Activities

All the newly synthesized derivatives of triazole-based thiosemicarbazone (**6a–u**) were screened in vitro for inhibition of acetylcholinesterase (AChE) and butyrylcholinesterase (BuChE) activities. All the newly afforded derivatives, except **6c** and **6d**, which are found to be inactive, displayed good to moderate inhibition, with IC₅₀ ranging from 0.10 ± 0.050 to 12.20 ± 0.30 μM against AChE and 0.20 ± 0.050 μM to 14.10 ± 0.40 μM against BuChE compared to the standard drug donepezil, which exhibited IC₅₀ of 2.16 ± 0.12 and 4.5 ± 0.11 μM against AChE and BuChE, respectively (Table 1). A structure–activity relationship (SAR) based on substituent/s and electron donating/withdrawing effects on phenyl rings B and C was developed. The compounds were divided into five major parts: triazole moiety, ring A, thiosemicarbazone moiety, ring B, and ring C. Each part of the synthesized compounds was found to be actively participating in inhibition of both acetylcholinesterase (AChE) and butyrylcholinesterase (BuChE). Furthermore, it was determined that by keeping the triazole, ring A, and thiosemicarbazone moieties constant, the variation in inhibitory potentials was determined by attachment of substituents of diverse nature at various positions in different number/s around both rings B and C (Figure 4, Table 1).

Structure–Activity Relationship (SAR) for Inhibition of Acetylcholinesterase (AChE) and Butyrylcholinesterase (BuChE)

Analogue **6i** with IC₅₀ = 0.10 ± 0.050 (for AChE) and IC₅₀ = 0.20 ± 0.050 μM (for BuChE) having di-substitutions (2-nitro, 3-hydroxy groups) at ring B and tri-substitutions (2-nitro, 4,5-dichloro groups) at ring C emerged as the most active inhibitor of targeted AChE and BuChE enzymes, whereas analogue **6b** (IC₅₀ = 0.20 ± 0.10 μM for AChE) (IC₅₀ = 0.30 ± 0.10 μM for BuChE) having di-Cl at 4,5- and —NO₂ groups at 2-position of phenyl ring B and hydroxy group at *ortho*-position of phenyl ring C was recognized as the second-most active among the current synthesized series (Table 1). The greater number of attached electron-withdrawing groups, such as di-Cl and —NO₂ groups around ring C, as well as the presence of substituents (—OH) capable of forming hydrogen bonds with the active residue of amino acids of these analogues were responsible for enhanced inhibitory potentials for both targeted AChE and BuChE. The majority of the electronic density is removed from Ph-ring B and C by these di-Cl and —NO₂ groups, making it electron-deficient and further regaining stability through interactions with the active sites of targeted AChE and BuChE enzymes. The derivative **6k**, which has a *para*-bromo substitution on ring B and a *para*-tolyl group at 4-position of aryl ring C, was shown to have the least inhibitory activity against AChE and BuChE enzymes with IC₅₀ values of 12.20 ± 0.30 and 14.10 ± 0.40 μM. This reduced the potency of derivative **6k**, caused by the greater size of the attached substituent(s), which increased the crowdedness around both rings B and C and thus reduced the chance of interactions with catalytic residues of targeted enzymes (Table 1).

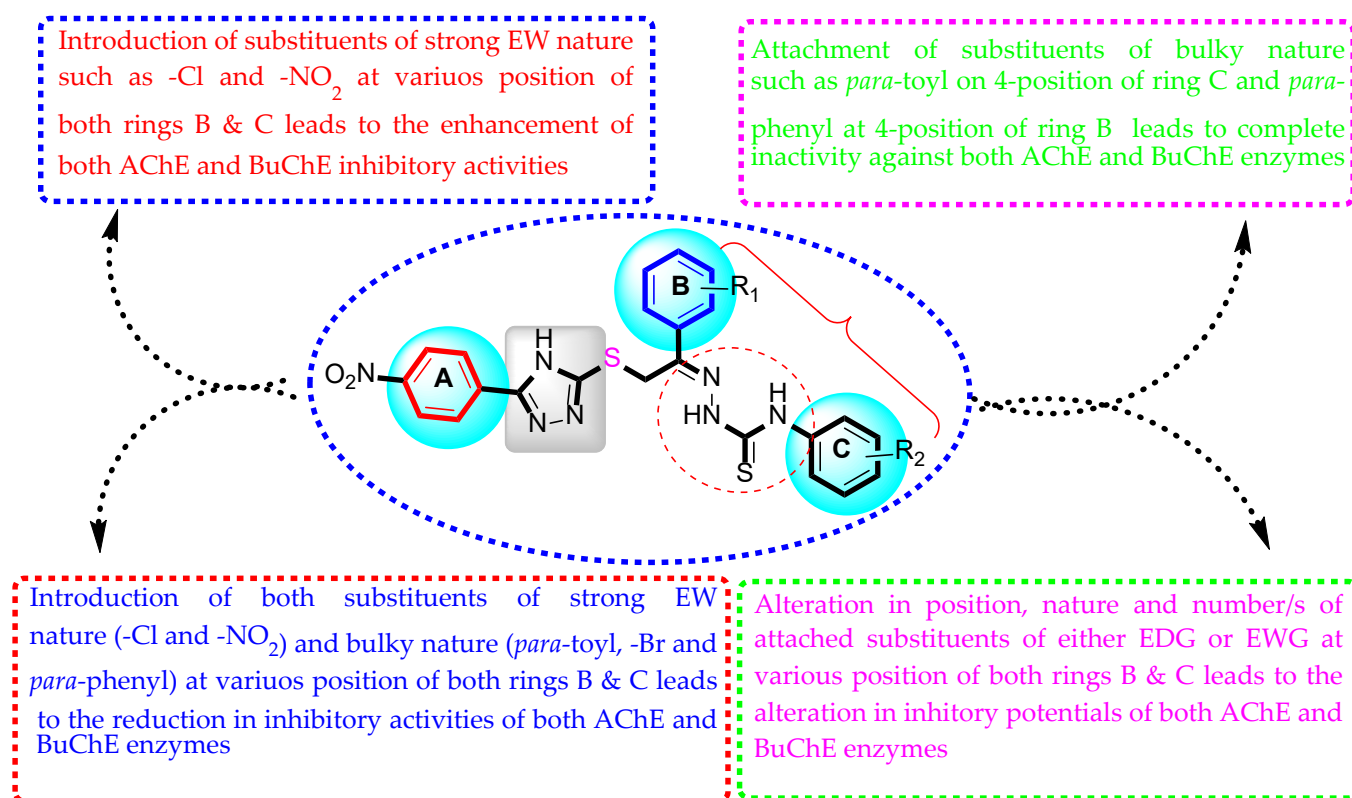


Figure 4. Summary of SAR studies of triazole-based thiosemicarbazone derivatives (6a–u).

Derivatives **6a**, **6b** and **6l** containing di-Cl groups at meta- and para-position and nitro group at ortho-position of ring C and a variety of other groups, including Br, OH, NO₂ and CH₃, at various positions of ring B, improved inhibition of activities of both AChE and BuChE enzymes. Among these three derivatives, derivative **6b** (IC₅₀ = 0.20 ± 0.10 and 0.30 ± 0.10 μM) with hydroxy group at ortho-position on ring B along with tri-substitutions (2-nitro and 3,4-di-Cl groups) at aryl ring C displayed superior inhibition of AChE and BuChE, compared to derivative **6a** (IC₅₀ = 5.10 ± 0.20 and 6.40 ± 0.20 μM), which had a bromo group at ortho-position of ring B and derivative **6l** (IC₅₀ = 4.60 ± 0.010 and 5.90 ± 0.10 μM), bearing NO₂ at ortho and CH₃ groups at para on ring B along with di-Cl groups at meta- and para-position and nitro group at ortho-position of ring C (Table 1). These three derivatives contain tri-substitutions (2-nitro, 3,4-dichloro groups) at ring C, but have different substituents (Br, OH, CH₃ and NO₂ groups) around ring B. This diverse nature of substituents around ring B have different tendencies to interact with active site of targeted enzymes and hence cause variation in inhibitory potentials of these three derivatives (Table 1). Moreover, derivative **6a** which contains a bromo at ortho on ring B and di-Cl groups at meta- and para-position and nitro group at ortho-position of ring C, exhibits better inhibition of AChE and BuChE activities than derivative **6h**, which has a bromo moiety at para on ring B and ortho-nitro and para-methyl substitutions on ring C, might be due to di-Cl groups on ring, as well as different position of bromo moiety around ring B (Table 1).

Derivative **6g** (IC₅₀ = 2.10 ± 0.10 and 4.30 ± 0.10 μM), containing two methoxy groups at ortho- and meta-position of ring B and a nitro group at the para-position of the phenyl ring C, exhibited better inhibition of AChE and BuChE activities, compared to derivative **6f** (IC₅₀ = 2.40 ± 0.10 and 4.70 ± 0.10 μM), which had two methoxy groups at the ortho- and meta-positions of ring B and ortho-nitro and para-methyl groups on phenyl ring C (Table 1). This enhanced inhibition of AChE and BuChE activities of derivative **6g** might be due to the stronger electron withdrawing nature of nitro group, making the ring C partially positive, which further established a pi-cation interaction with the active enzyme site. Alternatively,

derivative **6f** had both electron-donating (CH_3) and electron-withdrawing (NO_2) groups on ring C, which did not create charge on ring C and hence resulted in lesser activities of AChE and BuChE (Table 1).

Comparing derivative **6h** ($\text{IC}_{50} = 9.10 \pm 0.20$ and $11.20 \pm 0.30 \mu\text{M}$), which has a bromo group at the para position of the phenyl ring B and a nitro group at ortho-position and a methyl group at the para-position of the phenyl ring C, with derivatives **6m** ($\text{IC}_{50} = 2.70 \pm 0.10$ and $3.80 \pm 0.10 \mu\text{M}$) having di-Cl groups at meta- and para-positions of ring B and nitro group at ortho-position and methyl group at para-position on phenyl ring C and **6r** ($\text{IC}_{50} = 1.30 \pm 0.050$ and $2.20 \pm 0.10 \mu\text{M}$) having nitro group at ortho on ring B and nitro group at ortho-position and methyl group at para-position on phenyl ring C and **6t** ($\text{IC}_{50} = 1.90 \pm 0.10$ and $2.50 \pm 0.10 \mu\text{M}$) with a methoxy group at meta-position of ring B and the nitro group at ortho-position and the methyl group at para-position on phenyl ring C (Table 1). The small difference in the inhibitory activities (AChE and BuChE) of all derivatives might be due to the different nature and position of the substituent/s on phenyl ring B (Table 1).

Derivative **6n** ($\text{IC}_{50} = 0.70 \pm 0.05$ and $1.70 \pm 0.050 \mu\text{M}$), which has di-chloro groups at meta- and para-positions on ring B and a nitro group at para-position on ring C, with derivative **6s** ($\text{IC}_{50} = 1.40 \pm 0.050$ and $2.30 \pm 0.10 \mu\text{M}$), which has a nitro group at ortho position on ring B and nitro moiety at para position on ring C, and derivative **6u** ($\text{IC}_{50} = 2.90 \pm 0.10$ and $3.70 \pm 0.10 \mu\text{M}$), with a methoxy group at the meta-position on ring B and nitro moiety at the para position on ring C were compared (Table 1). Difference in the inhibitory activities (AChE and BuChE) of these derivatives might be due to the different nature and position of substituent/s on ring B (Table 1). Number, nature, position and electron-donating/withdrawing nature of substituents considerably influenced inhibition of activities.

2.3. Docking Study

Molecular docking was analyzed in order to gain an understanding of the binding mechanism of synthesized compounds against both the targeted enzymes. The optimized compounds were docked based on the co-crystal of each crystallographic structure. Each compound was assigned a total of 30 conformations prior to the docking process. For further investigation, the top-ranked conformations of potent compounds were chosen. The docking results revealed that all the compounds were well oriented in the active site of both enzymes. In general, we found that all of the compounds in the series—with different substituted groups at all three ends of the compound (according to the scheme), where one end has a nitro group, the second end has a halogen group, and the most important end (third) has a different substituted group—had inhibitory potential against the target. These typically belong to electron-withdrawing or electron-donating groups.

The protein–ligand interaction profile of the most active analogue, **6i**, had several key interactions with catalytic residues of acetylcholinesterase enzyme, including Tyr332 (pi-sigma and pi-pi stacked), Trp82 (pi-anion), Glu197 (HB), Phe329 (pi-sulfur), Ser198 (HB), His438 (HB), Asn289 (HB), Asn68 (HB) and Asp70 (pi-cation) (Figure 5), while against butyrylcholinesterase enzymes, it interacts through numerous interactions such as Tyr116 (pi-alkyl), Tyr130 (pi-alkyl), His440 (CHB), Phe330 (pi-anion), Asp72 (pi-cation), Asn85 (HB), Tyr121 (pi-sulfur), Trp279 (pi-pi shaped and amide-pi stacked), Tyr70 (HB), Tyr334 (pi-pi stacked), Trp84 (pi-pi T shaped stacked), Gly118 (HB) and Gly117 (pi-pi stacked) (Figure 6).

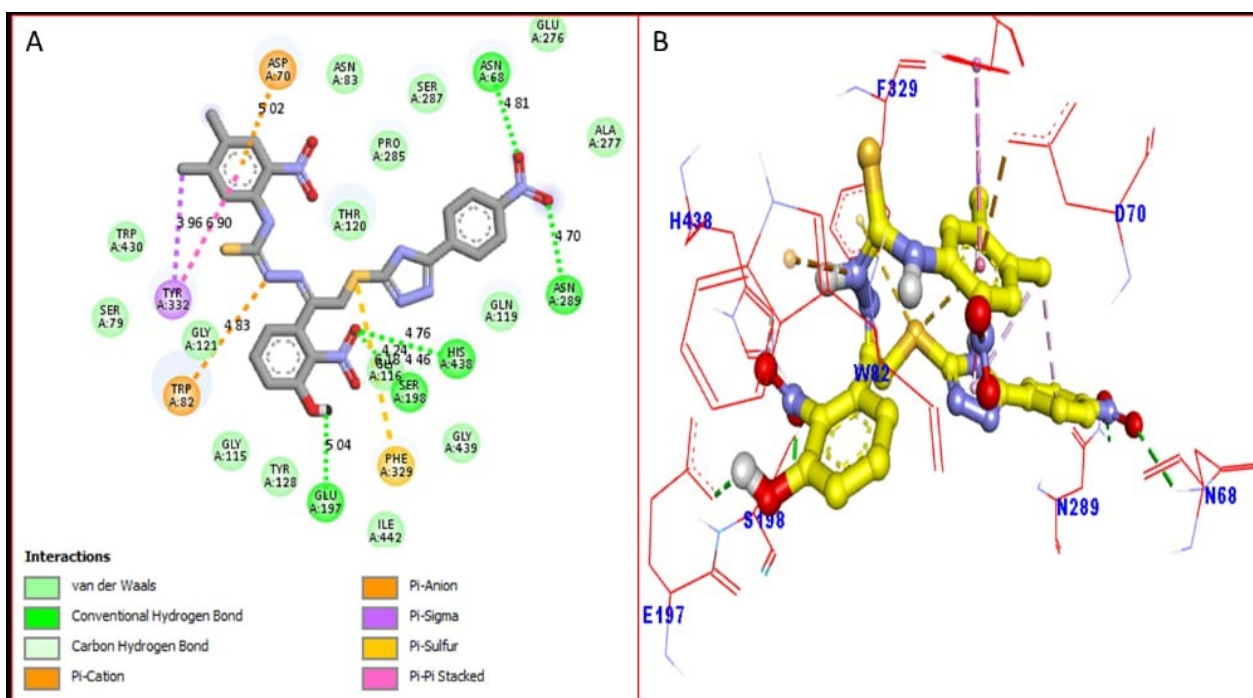


Figure 5. Protein–ligand interaction (PLI) profile of analogue **6i** against acetylcholinesterase (AChE): (A) 2D; (B) 3D.

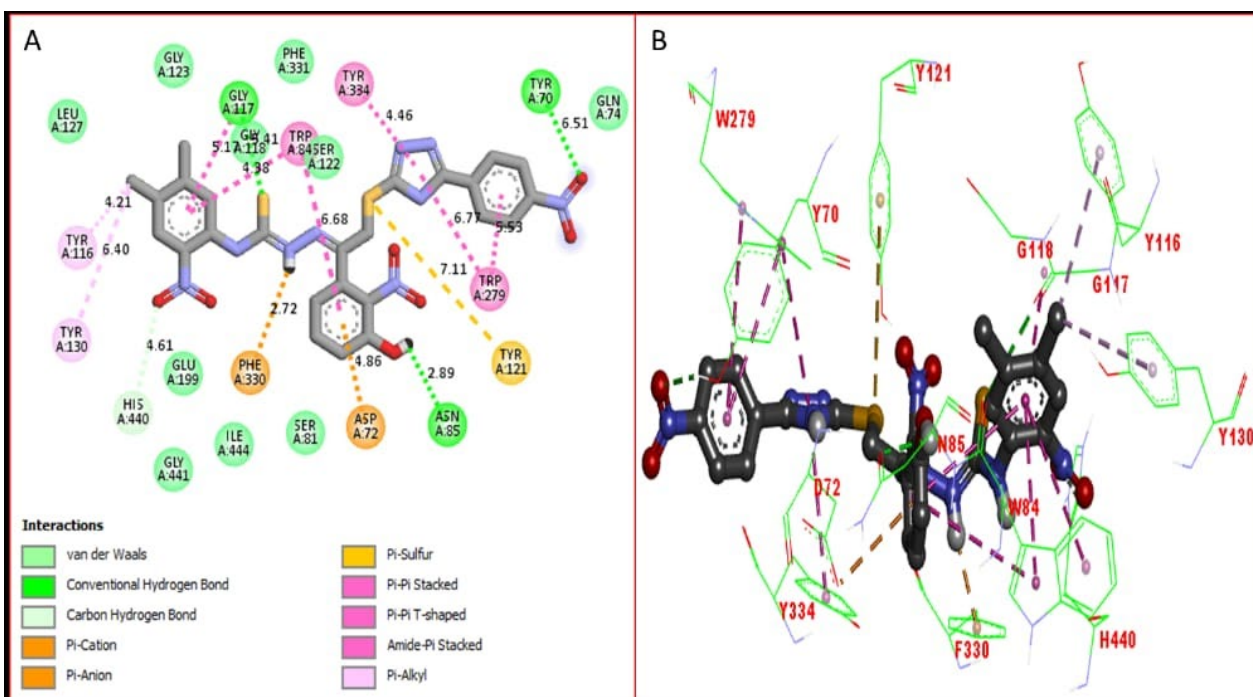


Figure 6. Protein–ligand interaction (PLI) profile of analogue **6i** against butyrylcholinesterase (BuChE): (A) 2D; (B) 3D.

As for the second-most active analogue, **6b**, the protein–ligand interaction (PLI) profile showed that this scaffold enhanced inhibitory potential against AChE by interacting with the active part of the AChE enzyme through several significant interactions, such as Gly118 (CHB), Gly117 (pi-pi stacked), Ile444 (pi-alkyl), Tyr130 (pi-alkyl), Trp84 (pi-sigma and pi-pi stacked), Phe330 (pi-donor HB), His440 (pi-alkyl), Tyr121 (HB), Tyr334 (pi-sulfur and amide-pi stacked), Tyr70 (HB and pi-pi T shaped), Trp279 (pi-pi T shaped), Ser122 (HB) and

Asp72 (pi-anion) (Figure 7), while against butyrylcholinesterase this analogue **6b** adopted numerous key interactions including Pro285 (HB), His438 (pi-alkyl), Phe329 (pi-sulfur and pi-alkyl), Ala328 (alkyl), Gly117 (HB), Gly116 (HB), Thr120 (pi-sigma), Trp82 (pi-pi stacked), Gly115 (HB) and Tyr128 (HB) (Figure 8).

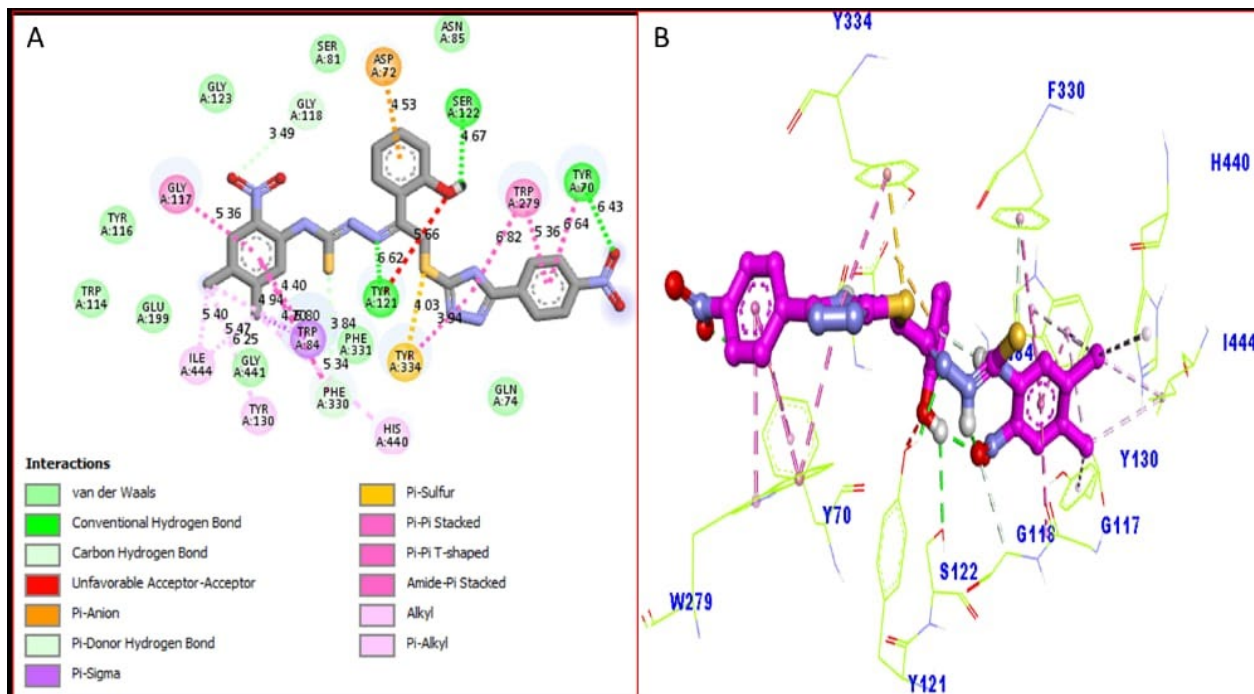


Figure 7. Protein–ligand interaction (PLI) profile of analogue **6b** against acetylcholinesterase (AChE): (A) 2D; (B) 3D.

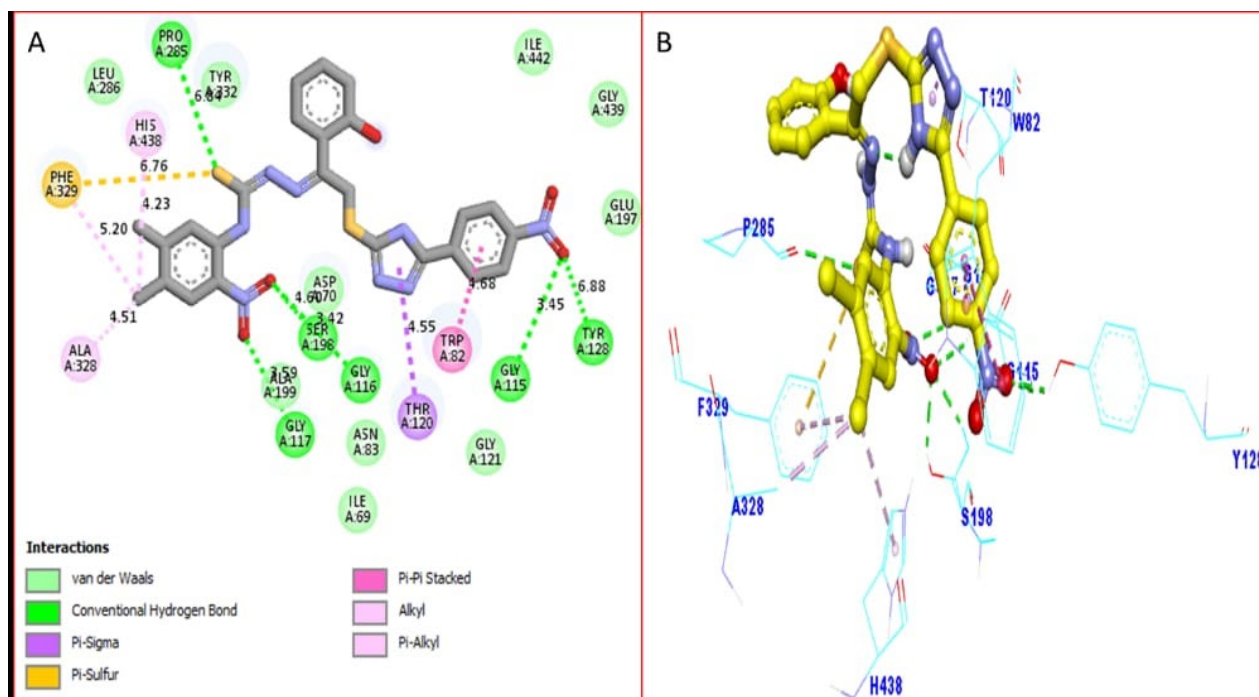


Figure 8. Protein–ligand interactions (PLI) profile of analogue **6b** against butyrylcholinesterase (BuChE): (A) 2D; (B) 3D.

The protein–ligand interaction (PLI) profile of the third-most active analogue, **6q**, showed that it established numerous interesting key interactions with active sites of the acetylcholinesterase enzyme, including Tyr128 (HB), Trp82 (pi-pi stacked), Trp430 (pi-alkyl), Tyr332 (pi-alkyl), Ala328 (pi-alkyl), pro285 (HB), Phe329 (pi-pi T shaped and pi-alkyl), Leu286 (pi-alkyl), Trp231 (pi-pi T shaped), Gly117 (HB), Ser198 (HB), Gly116 (HB), His438 (HB and pi-alkyl) and Asp70 (pi-anion) (Figure 9), while against the butyrylcholinesterase enzyme it established several important interactions, such as Tyr130 (HB), Tyr70 (pi-sulfur), Tyr338 (pi-pi T shaped), Arg289 (alkyl), Phe331 (pi-pi stacked and pi-sulfur), Trp279 (pi-pi stacked), Trp84 (pi-stacked), Phe330 (pi-pi stacked) and Gly117 (HB) as shown in (Figure 10).

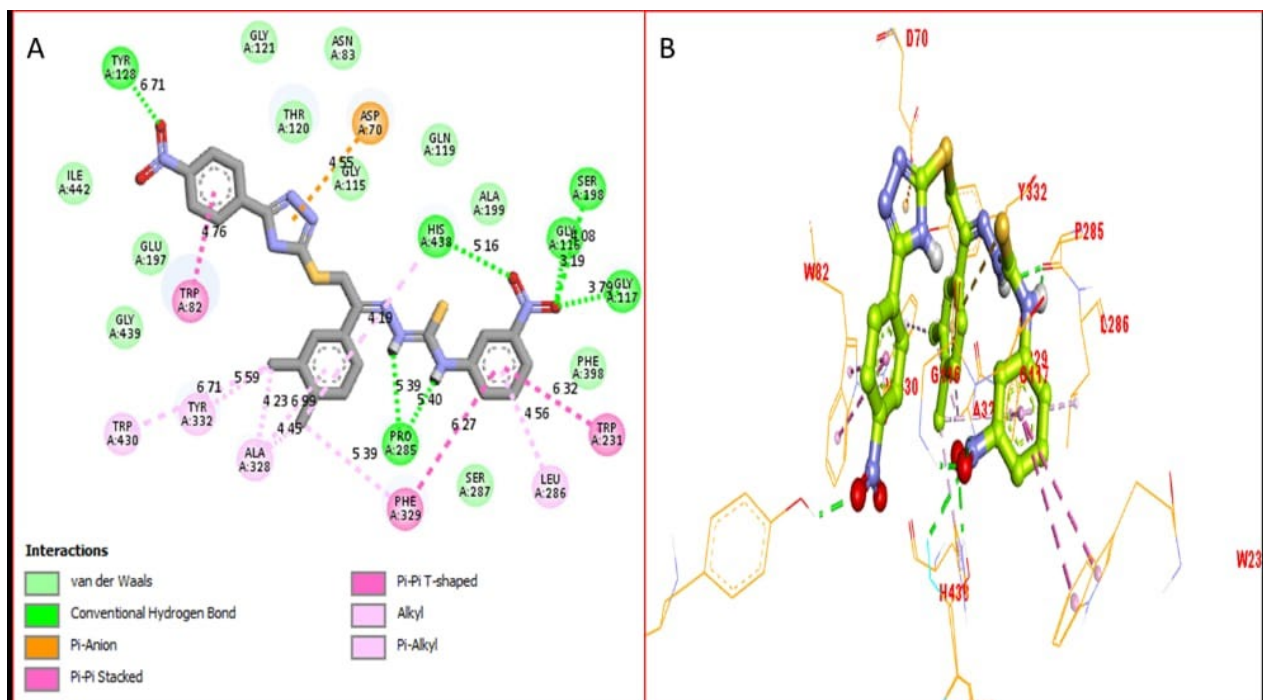


Figure 9. Protein–ligand interaction (PLI) profile of analogue **6q** against acetylcholinesterase (AChE): (A) 2D; (B) 3D.

Calculated binding energies, number of hydrogen bonds, and the number of closest residues surround the selected docked analogues into the active site of both AChE and BuChE enzymes are shown in Table 2.

Table 2. Binding energies, number of hydrogen bonding and the number of closest residues of the selected docked analogues into the active site of both AchE and BuChE.

Active Derivatives	Name of Enzyme	Free Binding Energy (kcal/mol)	Number of HBs	Number of Closest Residues
6i	AChE	−12.13	5	24
	BuChE	−11.78	2	22
6b	AChE	−11.37	3	22
	BuChE	−10.49	5	21
6q	AChE	−10.63	6	23
	BuChE	−9.42	3	24

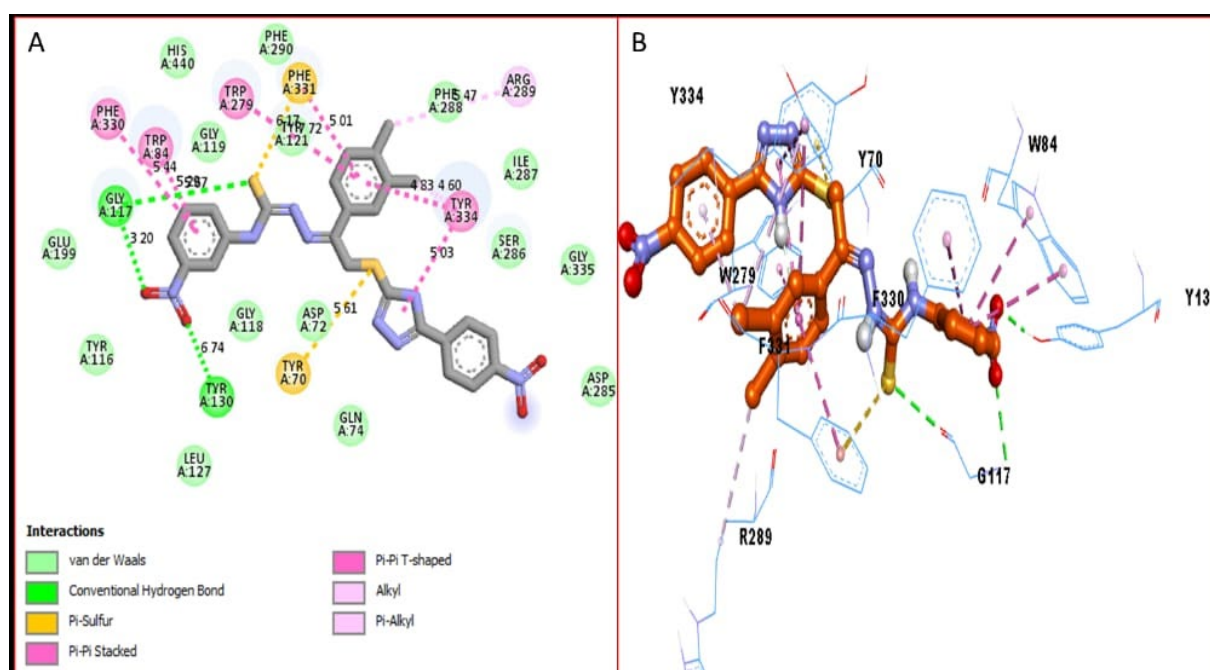


Figure 10. Protein–ligand interaction (PLI) profile of analogue **6q** against butyrylcholinesterase (BuChE): (A) 2D; (B) 3D.

3. Experimental

All chemicals and solvents were purchased from Sigma Aldrich (St. Louis, MO, USA) with a purity of 97 up to 99%.

3.1. General Procedure of 1,2,4-Triazole Bearing Thiosemicarbazone Derivatives (**6a–u**)

Thiosemicarbazide (**1**, 0.5 mmol) was treated with 4-nitrobenzoyl chloride (0.5 mmol) in DMF (10 mL) in the presence of triethylamine (0.5 mL) and refluxed for 3 h to yield 2-(4-nitrobenzoyl)hydrazine-1-carbothioamide as first intermediate (**2**), which further undergoes cyclization on stirring overnight in 2% aqueous solution of sodium hydroxide (10 mL followed by neutralization with dilute HCl (5 mL) to yield 1,2,4-triazole-3-thiole (**3**) as the second intermediate product. Intermediate (**3**) was then reacted with equivalent different substituted phenacyl bromide in ethanol (10 mL) in the presence of triethylamine (0.5 mL) and refluxed for 3 h to obtain third intermediate (**4**). Intermediate (**4**) was then mixed with hydrazine hydrate (5 mL) in methanol (10 mL) in the presence of a few drops of glacial acetic acid to give fourth intermediate (**5**). Finally intermediate (**5**) was treated with equivalent different substituted isothiocyanate in tetrahydrofuran (10 mL) in the presence of triethylamine (0.5 mL) and the resulting mixture was stirred under reflux until the conversion was completed (monitored by TLC, reflux 6–8 h). After being cooled to room temperature, it was reacted with 5% Na₂S₂O₃ (20 mL) and extracted with CH₂Cl₂/MeOH (10:1, 10 mL × 4). The combined organic layer was dried over anhydrous sodium sulfate and concentrated. The given residue was purified through silica gel column chromatography using a mixture of petroleum ether and EtOAc as eluent to yield the desired triazole-based thiosemicarbazone derivatives (**6a–u**).

3.2. Spectral Analysis

All the proton NMR spectra are shown in Supplementary Materials.

3.2.1. (.E)-2-(1-(2-bromophenyl)-2-((5-(4-nitrophenyl)-4H-1,2,4-triazol-3-yl)thio)ethylidene)-N-(4,5-dichloro-2-nitrophenyl)hydrazine-1-carbothioamide (**6a**)

Yield: 63%; ¹H NMR (600 MHz, DMSO-*d*₆): δ 13.25 (s, 1H, NH), 11.81 (s, 1H, NH), 10.11 (s, 1H, NH), 8.28 (s, 1H, Ar-H), 8.10 (s, 1H, Ar-H), 7.88 (d, *J* = 8.88 Hz, 2H, Ar-H), 7.79

(d, $J = 8.46$ Hz, 2H, Ar-H), 7.43 (t, $J = 7.92$ Hz, 2H, Ar-H), 7.27 (t, $J = 7.68$ Hz, 1H, Ar-H), 7.04 (d, $J = 7.56$ Hz, 1H, Ar-H), 2.34 (s, 2H, S-CH₂). ¹³C NMR (150 MHz, DMSO-*d*₆): δ 184.0, 158.5, 157.3, 155.4, 147.5, 146.2, 138.4, 137.1, 135.2, 134.4, 132.5, 131.6, 130.0, 129.0, 127.5, 126.8, 126.8, 126.3, 125.5, 124.1, 124.1, 122.0, 31.0. HRMS (ESI) m/z : [M+H]⁺ calcd for C₂₃H₁₆BrCl₂N₈O₄S₂, 680.8117; Found, 680.8100.

3.2.2. (.E)-N-(4,5-dichloro-2-nitrophenyl)-2-(1-(2-hydroxyphenyl)-2-((5-(4-nitrophenyl)-4H-1,2,4-triazol-3-yl)thio)ethylidene)hydrazine-1-carbothioamide (**6b**)

Yield: 72%; ¹H NMR (600 MHz, DMSO-*d*₆): δ 13.39 (s, 1H, NH), 13.27 (s, 1H, NH), 12.01 (s, 1H, NH), 10.15 (s, 1H, OH), 8.91 (s, 1H, Ar-H), 8.30 (s, 1H, Ar-H), 8.16-7.87 (m, 4H, Ar-H), 7.83-7.72 (m, 2H, Ar-H), 7.45 (t, $J = 7.74$ Hz, 1H, Ar-H), 7.25 (t, $J = 7.74$ Hz, 1H, Ar-H), 2.28 (s, 2H, S-CH₂). ¹³C NMR (150 MHz, DMSO-*d*₆): δ 183.9, 162.5, 158.4, 157.2, 155.3, 147.4, 146.4, 138.3, 137.2, 132.4, 132.1, 131.5, 129.2, 127.1, 127.1, 126.4, 125.5, 124.1, 124.1, 121.0, 118.3, 117.0, 32.0. HRMS (ESI) m/z : [M+H]⁺ calcd for C₂₃H₁₇Cl₂N₈O₅S₂, 619.0150; Found, 619.0134.

3.2.3. (.E)-2-(1-([1,1'-biphenyl]-4-yl)-2-((5-(4-nitrophenyl)-4H-1,2,4-triazol-3-yl)thio)ethylidene)-N-phenylhydrazine-1-carbothioamide (**6c**)

Yield: 75%; ¹H NMR (600 MHz, DMSO-*d*₆): δ 13.36 (s, 1H, -NH), 11.25 (s, 1H, -NH), 11.08 (s, 1H, -NH), 8.23 (d, $J = 9.1$ Hz, 2H, Ar-H), 7.99 (d, $J = 9.1$ Hz, 2H, Ar-H), 7.96 (d, $J = 8.4$ Hz, 2H, Ar-H), 7.86 (dd, $J = 7.3$ Hz, 2H, Ar-H), 7.72 (dd, $J = 7.8$ Hz, 1.9 Hz, 2H, Ar-H), 7.63-7.56 (m, 5H, Ar-H), 7.40-7.35 (m, 2H, Ar-H), 7.06-6.98 (m, 1H, Ar-H), 3.73 (s, 2H, S-CH₂). ¹³C NMR (150 MHz, DMSO-*d*₆): δ 183.8, 158.4, 157.2, 155.2, 147.5, 142.7, 140.4, 138.2, 138.1, 132.5, 129.3, 129.3, 128.8, 128.8, 128.6, 128.6, 128.0, 127.6, 127.6, 127.5, 127.5, 127.2, 126.6, 126.6, 126.1, 126.1, 124.0, 124.0, 31.4. HRMS (ESI) m/z : [M+H]⁺ calcd for C₂₉H₂₄N₇O₂S₂, 566.1429; Found, 566.1408.

3.2.4. (.E)-2-(1-([1,1'-biphenyl]-4-yl)-2-((5-(4-nitrophenyl)-4H-1,2,4-triazol-3-yl)thio)ethylidene)-N-(4'-methyl-[1,1'-biphenyl]-4-yl)hydrazine-1-carbothioamide (**6d**)

Yield: 73%; ¹H NMR (600 MHz, DMSO-*d*₆): δ 13.38 (s, 1H, -NH), 11.24 (s, 1H, -NH), 11.07 (s, 1H, -NH), 8.22 (d, $J = 6.8$ Hz, 2H, Ar-H), 7.98 (d, $J = 8.6$ Hz, 2H, Ar-H), 7.95 (d, $J = 7.2$ Hz, 2H, Ar-H), 7.85 (dd, $J = 7.8$ Hz, 2H, Ar-H), 7.78-7.69 (m, 5H, Ar-H), 7.67 (d, $J = 7.6$ Hz, 2H, Ar-H), 7.63 (d, $J = 7.3$ Hz, 2H, Ar-H), 7.30 (d, $J = 6.6$ Hz, 2H, Ar-H), 7.12 (d, $J = 6.7$ Hz, 2H, Ar-H), 3.71 (s, 2H, S-CH₂), 2.31 (s, 3H, -CH₃). ¹³C NMR (150 MHz, DMSO-*d*₆): δ 183.7, 158.3, 57.1, 155.1, 147.4, 142.6, 140.3, 139.3, 138.1, 137.3, 136.9, 132.4, 131.3, 130.1, 129.2, 129.2, 129.0, 129.0, 128.7, 128.7, 127.7, 127.7, 127.5, 127.5, 127.4, 127.4, 127.3, 127.3, 127.1, 126.5, 126.5, 124.1, 124.1, 123.9, 123.9, 20.8; HRMS (ESI) m/z : [M+H]⁺ calcd for C₃₆H₃₀N₇O₂S₂, 656.1898; Found, 656.1877.

3.2.5. (.E)-2-(1-([1,1'-biphenyl]-4-yl)-2-((5-(4-nitrophenyl)-4H-1,2,4-triazol-3-yl)thio)ethylidene)-N-(3-nitrophenyl)hydrazine-1-carbothioamide (**6e**)

Yield: 83%; ¹H NMR (600 MHz, DMSO-*d*₆): δ 13.35 (s, 1H, -NH), 11.31 (s, 1H, -NH), 11.14 (s, 1H, -NH), 8.58 (dd, $J = 2.4$ Hz, 2.0 Hz, 1H, Ar-H), 8.29 (d, $J = 9.0$ Hz, 2H, Ar-H), 8.05 (d, $J = 9.2$ Hz, 2H, Ar-H), 8.02 (d, $J = 8.5$ Hz, 2H, Ar-H), 7.94 (dd, $J = 7.5$ Hz, 2H, Ar-H), 7.92-7.87 (m, 1H, Ar-H), 7.85-7.79 (m, 1H, Ar-H), 7.75-7.63 (m, 5H, Ar-H), 7.60 (t, $J = 8.6$ Hz, 1H, Ar-H), 3.79 (s, 2H, S-CH₂). ¹³C NMR (150 MHz, DMSO-*d*₆): δ 184.0, 158.6, 157.4, 155.4, 148.0, 147.7, 142.9, 140.6, 137.8, 136.4, 132.7, 132.4, 129.7, 129.5, 129.5, 129.0, 129.0, 127.8, 127.8, 127.7, 127.7, 127.4, 126.8, 126.8, 124.2, 124.2, 119.7, 119.2, 31.6. HRMS (ESI) m/z : [M+H]⁺ calcd for C₂₉H₂₃N₈O₄S₂, 611.1176; Found, 611.1159.

3.2.6. (.E)-2-(1-(2,5-dimethoxyphenyl)-2-((5-(4-nitrophenyl)-4H-1,2,4-triazol-3-yl)thio)ethylidene)-N-(4-methyl-2-nitrophenyl)hydrazine-1-carbothioamide (**6f**)

Yield: 80%; ¹H NMR (600 MHz, DMSO-*d*₆): δ 13.33 (s, 1H, -NH), 11.15 (s, 1H, -NH), 10.81 (s, 1H, -NH), 8.85 (d, $J = 6.9$ Hz, 1H, Ar-H), 8.33 (d, $J = 2.1$ Hz, 1H, Ar-H), 8.28 (d,

$J = 9.3$ Hz, 2H, Ar-H), 8.05 (d, $J = 9.0$ Hz, 2H, Ar-H), 7.42 (d, $J = 2.0$ Hz, 1H, Ar-H), 7.06 (d, $J = 7.1$ Hz, 1H, Ar-H), 7.98 (dd, $J = 7.1$ Hz, 1.5 Hz, 1H, Ar-H), 7.01 (dd, $J = 7.9$ Hz, 1.7 Hz, 1H, Ar-H), 3.74 (s, 2H, S-CH₂), 2.41 (s, 3H, CH₃), 3.92 (s, 3H, -OCH₃), 3.79 (s, 3H, -OCH₃). ¹³C NMR (150 MHz, DMSO-*d*₆): δ 184.1, 158.7, 157.5, 155.5, 152.9, 152.6, 147.8, 147.1, 138.5, 135.3, 135.2, 129.3, 126.9, 126.9, 125.2, 124.6, 124.2, 124.2, 118.1, 117.5, 115.3, 114.1, 32.0, 58.6, 58.3, 20.2. HRMS (ESI) m/z : [M+H]⁺ calcd for C₂₆H₂₅N₈O₆S₂, 609.1334; Found, 609.1320.

3.2.7. (.E)-2-(1-(2,5-dimethoxyphenyl)-2-((5-(4-nitrophenyl)-4H-1,2,4-triazol-3-yl)thio)ethylidene)-N-(4-nitrophenyl)hydrazine-1-carbothioamide (**6g**)

Yield: 80%; ¹H NMR (600 MHz, DMSO-*d*₆): δ 13.36 (s, 1H, -NH), 11.16 (s, 1H, -NH), 10.80 (s, 1H, -NH), 8.27 (d, $J = 9.1$ Hz, 2H, Ar-H), 8.18 (d, $J = 6.9$ Hz, 2H, Ar-H), 8.04 (d, $J = 9.3$ Hz, 2H, Ar-H), 7.74 (d, $J = 6.8$ Hz, 2H, Ar-H), 7.41 (d, $J = 2.2$ Hz, 1H, Ar-H), 7.07 (d, $J = 7.2$ Hz, 1H, Ar-H), 7.02 (dd, $J = 7.8$ Hz, 1.8 Hz, 1H, Ar-H), 3.73 (s, 2H, S-CH₂), 3.91 (s, 3H, -OCH₃), 3.78 (s, 3H, -OCH₃). ¹³C NMR (150 MHz, DMSO-*d*₆): δ 184.4, 159.0, 157.8, 155.8, 153.2, 152.9, 148.1, 144.8, 144.1, 138.8, 127.2, 127.2, 125.0, 125.0, 124.6, 124.6, 124.4, 124.4, 118.4, 117.8, 115.6, 114.5, 56.0, 55.6, 32.3. HRMS (ESI) m/z : [M+H]⁺ calcd for C₂₅H₂₃N₈O₆S₂, 595.1179; Found, 595.1157.

3.2.8. (.E)-2-(1-(4-bromophenyl)-2-((5-(4-nitrophenyl)-4H-1,2,4-triazol-3-yl)thio)ethylidene)-N-(4-methyl-2-nitrophenyl)hydrazine-1-carbothioamide (**6h**)

Yield: 79%; ¹H NMR (600 MHz, DMSO-*d*₆): δ 13.32 (s, 1H, -NH), 11.06 (s, 1H, -NH), 10.72 (s, 1H, -NH), 8.78 (d, $J = 7.0$ Hz, 1H, Ar-H), 8.28 (d, $J = 1.8$ Hz, 1H, Ar-H), 8.25 (d, $J = 9.5$ Hz, 2H, Ar-H), 8.01 (d, $J = 7.3$ Hz, 2H, Ar-H), 7.73 (d, $J = 7.6$ Hz, 2H, Ar-H), 7.91 (dd, $J = 8.3$ Hz, 1.5 Hz, 1H, Ar-H), 7.67 (dd, $J = 7.9$ Hz, 2H, Ar-H), 3.73 (s, 2H, S-CH₂), 2.40 (s, 3H, CH₃). ¹³C NMR (150 MHz, DMSO-*d*₆): δ 183.9, 158.5, 157.3, 155.3, 147.6, 146.9, 138.3, 135.1, 135.0, 132.7, 131.4, 131.4, 129.1, 128.3, 128.3, 126.7, 126.7, 125.1, 125.0, 124.3, 124.1, 124.1, 31.5, 20.1. HRMS (ESI) m/z : [M+H]⁺ calcd for C₂₄H₂₀BrN₈O₄S₂, 627.0227; Found, 627.0217.

3.2.9. (.E)-N-(4,5-dichloro-2-nitrophenyl)-2-(1-(3-hydroxy-2-nitrophenyl)-2-((5-(4-nitrophenyl)-4H-1,2,4-triazol-3-yl)thio)ethylidene)hydrazine-1-carbothioamide (**6i**)

Yield: 61%; ¹H NMR (600 MHz, DMSO-*d*₆): δ 13.39 (s, 1H, NH), 13.30 (s, 1H, NH), 12.21 (s, 1H, NH), 10.51 (s, 1H, -OH), 8.91 (s, 1H, Ar-H), 8.35 (s, 1H, Ar-H), 8.30 (d, $J = 9.62$ Hz, 1H, Ar-H), 8.27–8.03 (m, 1H, Ar-H), 7.91–7.85 (m, 1H, Ar-H), 7.83 (d, $J = 9.0$ Hz, 2H, Ar-H), 7.76 (d, $J = 8.52$ Hz, 2H, Ar-H), 2.34 (s, 2H, S-CH₂). ¹³C NMR (150 MHz, DMSO-*d*₆): δ 184.4, 158.3, 157.4, 155.2, 153.0, 148.6, 147.5, 139.2, 138.4, 137.1, 136.5, 136.0, 131.5, 129.0, 126.6, 126.6, 126.3, 125.5, 124.0, 124.0, 121.4, 117.9, 30.4. HRMS (ESI) m/z : [M+H]⁺ calcd for C₂₃H₁₅Cl₂N₉O₇S₂, 662.9611; Found, 664.9600.

3.2.10. (.E)-2-(1-([1,1'-biphenyl]-4-yl)-2-((5-(4-nitrophenyl)-4H-1,2,4-triazol-3-yl)thio)ethylidene)-N-(2,5-dichloro-4-(dimethylamino)phenyl)hydrazine-1-carbothioamide (**6j**)

Yield: 64%; ¹H NMR (600 MHz, DMSO-*d*₆): δ 13.64 (s, 1H, NH), 11.54 (s, 1H, NH), 10.12 (s, 1H, NH), 8.23 (s, 1H, Ar-H), 8.18 (s, 1H, Ar-H), 8.04 (d, $J = 7.26$ Hz, 4H, Ar-H), 7.99–7.92 (m, 4H, Ar-H), 7.64–7.59 (m, 5H, Ar-H), 4.03 (s, 6H, -CH₃), 2.51 (s, 2H, S-CH₂). ¹³C NMR (150 MHz, DMSO-*d*₆): δ 184.0, 158.5, 157.3, 155.2, 148.3, 147.5, 143.0, 140.6, 138.4, 134.2, 132.5, 129.6, 129.6, 129.0, 128.9, 128.9, 127.8, 127.8, 127.4, 127.4, 127.1, 127.1, 126.9, 126.9, 126.4, 124.2, 124.2, 120.6, 40.5, 40.5, 31.4. HRMS (ESI) m/z : [M+H]⁺ calcd for C₃₁H₂₇Cl₂N₈O₂S₂, 678.0719; Found, 678.0701.

3.2.11. (.E)-2-(1-(4-bromophenyl)-2-((5-(4-nitrophenyl)-4H-1,2,4-triazol-3-yl)thio)ethylidene)-N-(4'-methyl-[1,1'-biphenyl]-4-yl)hydrazine-1-carbothioamide (**6k**)

Yield: 73%; ¹H NMR (600 MHz, DMSO-*d*₆): δ 13.31 (s, 1H, -NH), 11.25 (s, 1H, -NH), 11.08 (s, 1H, -NH), 8.21 (d, $J = 6.9$ Hz, 2H, Ar-H), 7.97 (d, $J = 8.9$ Hz, 2H, Ar-H), 7.73 (d, $J = 7.3$ Hz, 2H, Ar-H), 7.59 (dd, $J = 8.8$ Hz, 2H, Ar-H), 7.68 (d, $J = 7.7$ Hz, 2H, Ar-H), 7.64 (d, $J = 7.4$ Hz, 2H, Ar-H), 7.31 (d, $J = 6.7$ Hz, 2H, Ar-H), 7.13 (d, $J = 6.8$ Hz, 2H, Ar-H), 3.72 (s,

2H, S-CH₂), 2.32 (s, 3H, -CH₃). ¹³C NMR (150 MHz, DMSO-*d*₆): δ 184.0, 158.6, 157.4, 155.4, 147.7, 139.6, 138.4, 137.6, 137.2, 132.8, 131.5, 131.5, 130.4, 129.3, 129.3, 128.4, 128.4, 128.0, 128.0, 127.6, 127.6, 126.8, 126.8, 125.2, 124.4, 124.4, 124.2, 124.2, 31.6, 21.1. HRMS (ESI) *m/z*: [M+H]⁺ calcd for C₃₀H₂₅BrN₇O₂S₂, 658.0689; Found, 658.0669.

3.2.12. (.E)-N-(4,5-dichloro-2-nitrophenyl)-2-(1-(4-methyl-2-nitrophenyl)-2-((5-(4-nitrophenyl)-4H-1,2,4-triazol-3-yl)thio)ethylidene)hydrazine-1-carbothioamide (**6l**)

Yield: 67%; ¹H NMR (600 MHz, DMSO-*d*₆): δ 13.62 (s, 1H, NH), 13.38 (s, 1H, NH), 10.12 (s, 1H, NH), 8.90 (s, 1H, Ar-H), 8.23 (s, 1H, Ar-H), 8.16 (s, 1H, Ar-H), 8.02 (d, *J* = 5.58 Hz, 1H, Ar-H), 7.87 (d, *J* = 8.46 Hz, 1H, Ar-H), 7.75 (d, *J* = 8.4 Hz, 2H, Ar-H), 7.61 (d, *J* = 8.34 Hz, 2H, Ar-H), 2.50 (s, 2H, S-CH₂), 1.91 (s, 3H, -CH₃). ¹³C NMR (150 MHz, DMSO-*d*₆): δ 184.0, 158.6, 157.4, 155.3, 147.5, 147.2, 146.5, 141.4, 138.4, 137.0, 135.1, 132.2, 131.6, 129.9, 129.0, 126.8, 126.8, 126.3, 125.4, 125.2, 124.2, 124.2, 30.5, 20.0. HRMS (ESI) *m/z*: [M+H]⁺ calcd for C₂₄H₁₈Cl₂N₉O₆S₂, 662.0130; Found, 662.0111.

3.2.13. (.E)-2-(1-(3,4-dichlorophenyl)-2-((5-(4-nitrophenyl)-4H-1,2,4-triazol-3-yl)thio)ethylidene)-N-(4-methyl-2-nitrophenyl)hydrazine-1-carbothioamide (**6m**)

Yield: 61%; ¹H NMR (600 MHz, DMSO-*d*₆): δ 13.43 (s, 1H, -NH), 11.06 (s, 1H, -NH), 10.71 (s, 1H, -NH), 8.79 (d, *J* = 7.1 Hz, 1H, Ar-H), 8.29 (d, *J* = 1.7 Hz, 1H, Ar-H), 8.24 (d, *J* = 9.4 Hz, 2H, Ar-H), 8.02 (d, *J* = 7.5 Hz, 2H, Ar-H), 7.90 (dd, *J* = 8.4 Hz, 1.2 Hz, 1H, Ar-H), 7.83 (d, *J* = 1.5 Hz, 1H, Ar-H), 7.80 (dd, *J* = 8.5 Hz, 1.9 Hz, 1H, Ar-H), 7.66 (d, *J* = 8.9 Hz, 1H, Ar-H), 3.72 (s, 2H, S-CH₂), 2.40 (s, 3H, CH₃). ¹³C NMR (150 MHz, DMSO-*d*₆): δ 184.5, 159.1, 157.9, 155.9, 148.2, 147.5, 138.9, 136.0, 135.7, 135.6, 134.1, 133.8, 130.9, 130.6, 129.7, 127.3, 127.3, 126.6, 125.6, 124.7, 124.7, 124.5, 32.1, 20.6; HRMS (ESI) *m/z*: [M+H]⁺ calcd for C₂₄H₁₉Cl₂N₈O₄S₂, 617.0341; Found, 617.0327.

3.2.14. (.E)-2-(1-(3,4-dichlorophenyl)-2-((5-(4-nitrophenyl)-4H-1,2,4-triazol-3-yl)thio)ethylidene)-N-(4-nitrophenyl)hydrazine-1-carbothioamide (**6n**)

Yield: 59%; ¹H NMR (600 MHz, DMSO-*d*₆): δ 13.30 (s, 1H, -NH), 11.21 (s, 1H, -NH), 11.01 (s, 1H, -NH), 8.28 (d, *J* = 8.8 Hz, 2H, Ar-H), 8.23 (d, *J* = 9.6 Hz, 2H, Ar-H), 8.03 (d, *J* = 7.8 Hz, 2H, Ar-H), 7.85 (d, *J* = 1.8 Hz, 1H, Ar-H), 7.81 (dd, *J* = 8.5 Hz, 2.7 Hz, 1H, Ar-H), 7.74 (d, *J* = 8.0 Hz, 2H, Ar-H), 7.68 (d, *J* = 9.0 Hz, 1H, Ar-H), 3.73 (s, 2H, S-CH₂). ¹³C NMR (150 MHz, DMSO-*d*₆): δ 184.5, 159.1, 157.9, 155.9, 148.2, 144.2, 144.9, 138.9, 136.0, 134.0, 133.8, 130.9, 130.6, 127.3, 127.3, 126.6, 124.7, 124.7, 124.5, 124.5, 125.1, 125.1, 32.1; HRMS (ESI) *m/z*: [M+H]⁺ calcd for C₂₃H₁₇Cl₂N₈O₄S₂, 603.0183; Found, 603.0169.

3.2.15. (.E)-2-(1-(3,4-dichlorophenyl)-2-((5-(4-nitrophenyl)-4H-1,2,4-triazol-3-yl)thio)ethylidene)-N-phenylhydrazine-1-carbothioamide (**6o**)

Yield: 62%; ¹H NMR (600 MHz, DMSO-*d*₆): δ 13.41 (s, 1H, -NH), 11.31 (s, 1H, -NH), 11.15 (s, 1H, -NH), 8.29 (d, *J* = 6.8 Hz, 2H, Ar-H), 7.97 (d, *J* = 6.4 Hz, 2H, Ar-H), 7.90 (dd, *J* = 8.6 Hz, 2.1 Hz, 1H, Ar-H), 7.88 (d, *J* = 1.9 Hz, 1H, Ar-H), 7.73 (d, *J* = 8.0 Hz, 1H, Ar-H), 7.70 (dd, *J* = 7.7 Hz, 1.5 Hz, 2H, Ar-H), 7.43–7.35 (m, 2H, Ar-H), 7.08–6.99 (m, 1H, Ar-H), 3.74 (s, 2H, S-CH₂). ¹³C NMR (150 MHz, DMSO-*d*₆): δ 184.4, 159.0, 157.8, 155.8, 148.1, 138.8, 138.7, 135.9, 133.9, 133.7, 130.8, 130.5, 129.2, 129.2, 128.6, 127.2, 127.2, 126.7, 126.7, 126.5, 124.6, 124.6, 32.0. HRMS (ESI) *m/z*: [M+H]⁺ calcd for C₂₃H₁₈Cl₂N₇O₂S₂, 558.0337; Found, 558.0326.

3.2.16. (.E)-2-(1-(3,4-dichlorophenyl)-2-((5-(4-nitrophenyl)-4H-1,2,4-triazol-3-yl)thio)ethylidene)-N-(4'-methyl-[1,1'-biphenyl]-4-yl)hydrazine-1-carbothioamide (**6p**)

Yield: 64%; ¹H NMR (600 MHz, DMSO-*d*₆): δ 13.42 (s, 1H, -NH), 11.23 (s, 1H, -NH), 11.06 (s, 1H, -NH), 8.21 (d, *J* = 7.9 Hz, 2H, Ar-H), 7.97 (d, *J* = 8.7 Hz, 2H, Ar-H), 7.67 (d, *J* = 7.7 Hz, 2H, Ar-H), 7.91 (dd, *J* = 8.5 Hz, 2.0 Hz, 1H, Ar-H), 7.89 (d, *J* = 1.8 Hz, 1H, Ar-H), 7.74 (d, *J* = 8.1 Hz, 1H, Ar-H), 7.64 (d, *J* = 7.4 Hz, 2H, Ar-H), 7.31 (d, *J* = 6.7 Hz, 2H, Ar-H), 7.13 (d, *J* = 6.8 Hz, 2H, Ar-H), 3.72 (s, 2H, S-CH₂), 2.30 (s, 3H, -CH₃). ¹³C NMR (150 MHz,

DMSO- d_6): δ 184.3, 158.6, 157.4, 155.4, 147.7, 139.6, 138.4, 137.6, 137.2, 135.4, 134.2, 133.3, 130.4, 130.2, 130.1, 129.3, 129.3, 128.0, 128.0, 127.6, 127.6, 126.8, 126.8, 126.1, 124.4, 124.4, 124.2, 124.2, 31.7, 21.1. HRMS (ESI) m/z : $[M+H]^+$ calcd for $C_{30}H_{24}Cl_2N_7O_2S_2$, 648.0806; Found, 648.0790.

3.2.17. (.E)-2-(1-(3,4-dichlorophenyl)-2-((5-(4-nitrophenyl)-4H-1,2,4-triazol-3-yl)thio)ethylidene)-N-(3-nitrophenyl)hydrazine-1-carbothioamide (**6q**)

Yield: 67%; 1H NMR (600 MHz, DMSO- d_6): δ 13.36 (s, 1H, -NH), 11.29 (s, 1H, -NH), 11.13 (s, 1H, -NH), 8.58 (dd, $J = 2.3$ Hz, 2.0 Hz, 1H, Ar-H), 8.27 (d, $J = 8.1$ Hz, 2H, Ar-H), 8.03 (d, $J = 9.4$ Hz, 2H, Ar-H), 7.93 (dd, $J = 8.4$ Hz, 2.6 Hz, 1H, Ar-H), 7.88 (d, $J = 1.9$ Hz, 1H, Ar-H), 7.83–7.78 (m, 1H, Ar-H), 7.73 (d, $J = 8.3$ Hz, 1H, Ar-H), 7.69–7.64 (m, 1H, Ar-H), 7.62 (t, $J = 8.7$ Hz, 1H, Ar-H), 3.79 (s, 2H, S-CH₂). ^{13}C NMR (150 MHz, DMSO- d_6): δ 184.4, 159.0, 157.8, 155.8, 148.4, 148.1, 138.8, 138.2, 135.9, 133.9, 133.7, 132.8, 130.8, 130.5, 130.1, 127.2, 127.2, 126.5, 124.6, 124.6, 120.1, 119.6, 32.0.; HRMS (ESI) m/z : $[M+H]^+$ calcd for $C_{23}H_{17}Cl_2N_8O_4S_2$, 603.0187; Found, 603.0162.

3.2.18. (.E)-N-(4-methyl-2-nitrophenyl)-2-(1-(2-nitrophenyl)-2-((5-(4-nitrophenyl)-4H-1,2,4-triazol-3-yl)thio)ethylidene)hydrazine-1-carbothioamide (**6r**)

Yield: 69%; 1H NMR (600 MHz, DMSO- d_6): δ 13.33 (s, 1H, -NH), 11.06 (s, 1H, -NH), 10.72 (s, 1H, -NH), 8.77 (d, $J = 7.1$ Hz, 1H, Ar-H), 8.29 (d, $J = 1.7$ Hz, 1H, Ar-H), 8.24 (d, $J = 9.6$ Hz, 2H, Ar-H), 8.14 (dd, $J = 7.8$ Hz, 2.9 Hz 1H, Ar-H), 8.07 (dd, $J = 7.5$ Hz, 2.6 Hz 1H, Ar-H), 8.02 (d, $J = 7.3$ Hz, 2H, Ar-H), 7.99–7.93 (m, 1H, Ar-H), 7.91 (dd, $J = 8.3$ Hz, 1.5 Hz, 1H, Ar-H), 7.66 (dt, $J = 8.5$ Hz, 1.8 Hz 1H, Ar-H), 3.73 (s, 2H, S-CH₂), 2.40 (s, 3H, CH₃). ^{13}C NMR (150 MHz, DMSO- d_6): δ 184.6, 159.2, 158.0, 156.0, 148.3, 147.6, 139.0, 137.7, 135.8, 135.7, 135.3, 132.3, 132.2, 129.8, 127.4, 127.4, 126.8, 125.8, 125.7, 124.8, 124.8, 124.6, 31.0, 20.7; HRMS (ESI) m/z : $[M+H]^+$ calcd for $C_{24}H_{20}N_9O_6S_2$, 594.0974; Found, 594.0960.

3.2.19. (.E)-N-(4-nitrophenyl)-2-(1-(2-nitrophenyl)-2-((5-(4-nitrophenyl)-4H-1,2,4-triazol-3-yl)thio)ethylidene)hydrazine-1-carbothioamide (**6s**)

Yield: 63%; 1H NMR (600 MHz, DMSO- d_6): δ 13.38 (s, 1H, -NH), 11.34 (s, 1H, -NH), 11.17 (s, 1H, -NH), 8.32 (d, $J = 9.4$ Hz, 2H, Ar-H), 8.19 (dd, $J = 9.0$ Hz, 2H, Ar-H), 8.12 (dd, $J = 6.8$ Hz, 1.9 Hz 1H, Ar-H), 8.08 (d, $J = 9.6$ Hz, 2H, Ar-H), 8.03 (dd, $J = 8.5$ Hz, 1.6 Hz 1H, Ar-H), 7.94–7.88 (m, 1H, Ar-H), 7.76 (d, $J = 7.8$ Hz, 2H, Ar-H), 7.64 (dt, $J = 8.3$ Hz, 1.7 Hz, 1H, Ar-H), 3.82 (s, 2H, S-CH₂). ^{13}C NMR (150 MHz, DMSO- d_6): δ 184.4, 159.0, 157.8, 155.8, 148.1, 144.8, 144.1, 138.8, 135.6, 134.5, 132.1, 132.0, 127.2, 127.2, 126.6, 125.6, 125.0, 125.0, 124.6, 124.6, 124.4, 124.4, 31.0. HRMS (ESI) m/z : $[M+H]^+$ calcd for $C_{23}H_{18}N_9O_6S_2$, 580.0818; Found, 580.0806.

3.2.20. (.E)-2-(1-(3-methoxyphenyl)-2-((5-(4-nitrophenyl)-4H-1,2,4-triazol-3-yl)thio)ethylidene)-N-(4-methyl-2-nitrophenyl)hydrazine-1-carbothioamide (**6t**)

Yield: 59%; 1H NMR (600 MHz, DMSO- d_6): δ 13.37 (s, 1H, -NH), 11.14 (s, 1H, -NH), 10.81 (s, 1H, -NH), 8.85 (d, $J = 7.7$ Hz, 1H, Ar-H), 8.35 (d, $J = 1.6$ Hz, 1H, Ar-H), 8.30 (d, $J = 9.4$ Hz, 2H, Ar-H), 8.06 (d, $J = 9.2$ Hz, 2H, Ar-H), 7.97 (dd, $J = 7.3$ Hz, 1.8 Hz, 1H, Ar-H), 7.65 (dt, $J = 7.7$ Hz, 2.3 Hz, 1H, Ar-H), 7.43 (dd, $J = 2.1$ Hz, 1.3 Hz, 1H, Ar-H), 7.34 (dd, $J = 6.3$ Hz, $J = 6.6$ Hz, 1H, Ar-H), 7.10–6.99 (m, 1H, Ar-H), 3.74 (s, 3H, -OCH₃), 3.80 (s, 2H, S-CH₂), 2.45 (s, 3H, CH₃). ^{13}C NMR (150 MHz, DMSO- d_6): δ 184.0, 160.5, 158.6, 157.4, 155.4, 147.7, 147.0, 138.4, 135.2, 135.1, 134.8, 129.6, 129.2, 126.8, 126.8, 125.1, 124.4, 124.2, 124.2, 120.3, 116.4, 113.1, 55.6, 31.6, 20.1. HRMS (ESI) m/z : $[M+H]^+$ calcd for $C_{25}H_{23}N_8O_5S_2$, 579.1229; Found, 579.1213.

3.2.21. (.E)-2-(1-(3-methoxyphenyl)-2-((5-(4-nitrophenyl)-4H-1,2,4-triazol-3-yl)thio)ethylidene)-N-(4-nitrophenyl)hydrazine-1-carbothioamide (**6u**)

Yield: 61%; 1H NMR (600 MHz, DMSO- d_6): δ 13.40 (s, 1H, -NH), 11.34 (s, 1H, -NH), 11.07 (s, 1H, -NH), 7.76 (d, $J = 6.9$ Hz, 2H, Ar-H), 8.33 (d, $J = 9.6$ Hz, 2H, Ar-H), 8.13 (dd,

$J = 8.8$ Hz, 2H, Ar-H), 8.08 (d, $J = 9.2$ Hz, 2H, Ar-H), 7.68 (dt, $J = 8.7$ Hz, $J = 2.7$ Hz, 1H, Ar-H), 7.44 (dd, $J = 2.2$ Hz, 1.4 Hz, 1H, Ar-H), 7.35 (dd, $J = 6.8$ Hz, 7.0 Hz, 1H, Ar-H), 7.13–6.95 (m, 1H, Ar-H), 3.81 (s, 3H, -OCH₃), 3.78 (s, 2H, S-CH₂). ¹³C NMR (150 MHz, DMSO-*d*₆): δ 184.5, 161.0, 159.1, 157.9, 155.9, 148.2, 144.9, 144.2, 138.9, 135.3, 130.1, 127.3, 127.3, 125.1, 125.1, 124.7, 124.7, 124.5, 124.5, 120.8, 116.9, 113.6, 56.1, 32.1. HRMS (ESI) m/z : [M+H]⁺ calcd for C₂₄H₂₁N₈O₅S₂, 565.1073; Found, 565.1055.

3.3. Molecular Docking Protocol

Molecular docking was studied using MOE software to understand the binding mode of synthesized compounds against both the targeted enzymes in order to triangulate in vitro and in silico results well. The crystal structures of both targets were retrieved from the RCSB protein databank using the PDB codes 1ACL for AChE and 1P0P for BuChE. Using the default MOE-Dock module parameters, the crystallographic structures and all synthesized compounds were protonated and energy was minimized, resulting in optimized enzyme and compound structures. After that, the optimized enzyme and compound structures were used in a docking study. Comprehensive details of the docking protocol are included in our previous investigations [33,34].

3.4. Acetylcholinesterase Activity Assay Protocol

Based on previously described methods, in vitro study of AChE inhibitory profile was calculated [35,36]. In order to make a stock solution, compounds being analyzed were dissolved in DMSO (1 mg/mL). In addition, the working solutions were also prepared by using serial dilution (1–100 μ g/mL). The solution of AChE enzyme (20 μ L; 0.1 U/mL), analogues being tested with different concentration and buffer of sodium phosphate (150 μ L; pH 8.0; 0.1 M) were preincubated appropriately at 25 °C. The process was initiated as DTNB (10 mM; 10 μ L) and AChEI (14 mM; 10 μ L) were accumulated. The resulting residue was mixed (by using cyclomixer) and put on incubation for 10 min at 25 °C. Instead of compounds being tested using 10 μ L DMSO, the absorbance against blank reading was calculated with a microplate reader at 410 nm. Using the given formula as given, inhibition and IC₅₀ values were measured in comparison to donepezil (0.01–100 μ g/mL) as the reference standard (Equation (1)).

$$\% \text{Inhibition} = \text{Absorbance of control} - \text{Absorbance of compound} \times \frac{100}{A_{\text{control}}} \quad (1)$$

By plotting a nonlinear graph between inhibition and concentration, IC₅₀ was calculated using GraphPad Prism 5.3.

3.5. Butyrylcholinesterase Activity Assay Protocol

In order to explore the inhibition profile of in vitro BuChE enzyme, a similar procedure was adopted. For measurement of BuChE activity, the solution containing BuChE enzyme was used [35,36].

4. Conclusions

Triazole-based thiosemicarbazone derivatives (**6a–u**) were synthesized and screened for potential to inhibit activities of acetylcholinesterase and butyrylcholinesterase enzymes. All the synthetic derivatives (except compounds **6c** and **6d**, which were found to be completely inactive) displayed moderate to good inhibitory activities having an IC₅₀ values ranging from 0.20 \pm 0.050 to 12.20 \pm 0.30 μ M (against AChE) and 0.40 \pm 0.050 to 14.10 \pm 0.40 μ M (against BuChE) compared to the standard drug donepezil (IC₅₀ = 2.16 \pm 0.12 (AChE) and 4.5 \pm 0.11 μ M (BuChE)). Among the series, derivative **6q** (IC₅₀ = 0.20 \pm 0.050 μ M) was the most potent inhibitor of acetylcholinesterase enzyme, while derivative **6o** (IC₅₀ = 0.40 \pm 0.050 μ M) was the most active inhibitor of butyrylcholinesterase enzyme. The binding interactions of most active compounds with the active site of enzymes were established with the help of molecular docking studies.

Supplementary Materials: The following supporting information can be downloaded at: <https://www.mdpi.com/article/10.3390/molecules28010021/s1>, Figure S1. Proton NMR spectrum of compound **6b**. Figure S2. Proton NMR spectrum of compound **6d**. Figure S3. Proton NMR spectrum of compound **6i**. Figure S4. Proton NMR spectrum of compound **6j**.

Author Contributions: Conceptualization, H.U. and F.R.; methodology, R.H.; software, S.K.; validation, M.A.A. (Mahmoud A. Abdelaziz); A.A.; N.Z. and F.S.A.; formal analysis, S.A.A.S. and M.T.; investigation, M.T.; resources, M.T. and F.R.; data curation, K.M.K. and N.I.; writing—original draft preparation, H.U. and F.R.; writing—review and editing, A.A.; M.I.S.; N.Z.; I.J.; R.I.; M.A.A. (Marzough Aziz Albalawi) and M.S.; visualization, M.S. and I.J.; supervision, F.R.; project administration, F.R. and H.U.; funding acquisition, M.A.A. (Mahmoud A. Abdelaziz); M.A.A. (Mahmoud A. Abdelaziz) and F.S.A. All authors have read and agreed to the published version of the manuscript.

Funding: This research received no external funding.

Data Availability Statement: Not applicable.

Conflicts of Interest: The authors declare no conflict of interest.

References

1. Adams, R.L.; Craig, P.L.; Parsons, O.A. Neuropsychology of dementia. *Neurol. Clin.* **1986**, *4*, 387–404. [[CrossRef](#)] [[PubMed](#)]
2. Aisen, P.S.; Davis, K.L. The search for disease-modifying treatment for Alzheimer's disease. *Neurology* **1997**, *48*, 35–41. [[CrossRef](#)] [[PubMed](#)]
3. Jann, M.W. Preclinical pharmacology of metrifonate. *Pharmacotherapy* **1998**, *18*, 55–67. [[PubMed](#)]
4. Massoulié, J.; Pezzementi, L.; Bon, S.; Krejci, E.; Vallette, F.M. Molecular and cellular biology of cholinesterases. *Prog. Neurobiol.* **1993**, *41*, 31–91. [[CrossRef](#)] [[PubMed](#)]
5. Mushtaq, G.; H-Greig, N.; A-Khan, J.; A-Kamal, M. Status of acetylcholinesterase and butyrylcholinesterase in Alzheimer's disease and type 2 diabetes mellitus. *CNS Neurol. Disord. Drug Targets* **2014**, *13*, 1432–1439. [[CrossRef](#)] [[PubMed](#)]
6. Ahmad, S.; Iftikhar, F.; Ullah, F.; Sadiq, A.; Rashid, U. Rational design and synthesis of dihydropyrimidine based dual binding site acetylcholinesterase inhibitors. *Bioorg. Chem.* **2016**, *69*, 91–101. [[CrossRef](#)]
7. Auld, D.S.; Kornecook, T.J.; Bastianetto, S.; Quirion, R. Alzheimer's disease and the basal forebrain cholinergic system: Relations to β -amyloid peptides, cognition, and treatment strategies. *Prog. Neurobiol.* **2002**, *68*, 209–245. [[CrossRef](#)]
8. Ecobichon, D.J.; Comeau, A.M. Pseudocholinesterases of mammalian plasma: Physicochemical properties and organophosphate inhibition in eleven species. *Toxicol. Appl. Pharmacol.* **1973**, *24*, 92–100. [[CrossRef](#)]
9. Rahim, F.; Ullah, H.; Taha, M.; Wadood, A.; Javed, M.T.; Rehman, W.; Nawaz, M.; Ashraf, M.; Ali, M.; Sajid, M.; et al. Synthesis and in vitro acetylcholinesterase and butyrylcholinesterase inhibitory potential of hydrazide-based Schiff bases. *Bioorg. Chem.* **2016**, *68*, 30–40. [[CrossRef](#)]
10. Cavalli, A.; Bolognesi, M.L.; Minarini, A.; Rosini, M.; Tumiatti, V.; Recanatini, M.; Melchiorre, C. Multi-target-directed ligands to combat neurodegenerative diseases. *J. Med. Chem.* **2008**, *51*, 347–372. [[CrossRef](#)]
11. Rockwood, K.; Mintzer, J.; Truyen, L.; Wessel, T.; Wilkinson, D. Effects of a flexible galantamine dose in Alzheimer's disease: A randomised, controlled trial. *J. Neurol. Neurosurg. Psychiatry* **2001**, *71*, 589–595. [[CrossRef](#)] [[PubMed](#)]
12. Kucukguzel, I.; Kucukguzel, S.G.; Rollas, S.; Otuk-Sanis, G.; Ozdemir, O.; Bayrak, I.; Altug, T.; Stables, J.P. Synthesis of some 3-(arylalkylthio)-4-alkyl/aryl-5-(4-aminophenyl)-4H-1,2,4-triazole derivatives and their anticonvulsant activity. *Farmaco* **2004**, *59*, 893–901. [[CrossRef](#)]
13. Maddila, S.; Gorle, S.; Singh, M.; Lavanya, P.; Jonnalagadda, S.B. Synthesis and Anti-Inflammatory Activity of Fused 1,2,4-triazolo-[3,4-b][1,3,4]thiadiazole Derivatives of Phenothiazine. *Lett. Drug Des. Discov.* **2013**, *10*, 977. [[CrossRef](#)]
14. Almasirad, A.; Tabatabai, S.A.; Faizi, M.; Kebriaeezadeh, A.; Mehrabi, N.; Dalvandi, A.; Shafiee, A.; Ainsworth, C.; Easton, N.R.; Livezey, M.; et al. Synthesis and anticonvulsant activity of new 2-substituted-5-[2-(2-fluorophenoxy) phenyl]-1,3,4-oxadiazoles and 1,2,4-triazoles. *Bioorg. Med. Chem. Lett.* **2004**, *14*, 6057–6059. [[CrossRef](#)] [[PubMed](#)]
15. Maddila, S.; Pagadala, R.; Sreekanth, R.; Jonnalagadda, B. 1,2,4-Triazoles: A Review of Synthetic Approaches and the Biological Activity. *Lett. Org. Chem.* **2013**, *10*, 693–714. [[CrossRef](#)]
16. Oh, K.; Yamada, K.; Asami, T.; Yoshizawa, Y. Synthesis of novel brassinosteroid biosynthesis inhibitors based on the ketoconazole scaffold. *Bioorg. Med. Chem. Lett.* **2012**, *22*, 1625–1628. [[CrossRef](#)]

17. Wang, B.; Chu, D.; Feng, Y.; Shen, Y.; Aoyagi-Scharber, M.; Post, L.E. Discovery and Characterization of (8 S, 9 R)-5-Fluoro-8-(4-fluorophenyl)-9-(1-methyl-1 H-1, 2, 4-triazol-5-yl)-2, 7, 8, 9-tetrahydro-3 H-pyrido[4, 3, 2-de]phthalazin-3-one (BMN 673, Talazoparib), a Novel, Highly Potent, and Orally Efficacious Poly (ADP-ribose) Polymerase-1/2 Inhibitor, as an Anticancer Agent. *J. Med. Chem.* **2016**, *59*, 335–357.
18. Murphy, M.J.J. Molecular action and clinical relevance of aromatase inhibitors. *Oncologist* **1998**, *3*, 129–130. [[CrossRef](#)]
19. Borden, K.L.; Culjkovic-Kraljacic, B. Ribavirin as an anti-cancer therapy: Acute myeloid leukemia and beyond. *Leuk. Lymphoma.* **2010**, *51*, 1805–1815. [[CrossRef](#)]
20. Gomez-Junyent, J.; Benavent, E.; Sierra, Y.; el Haj, C.; Soldevila, L.; Torrejon, B.; Rigo-Bonnin, R.; Ariza, J.; Murillo, O. Efficacy of ceftolozane/tazobactam, alone and in combination with colistin, against multidrug-resistant *Pseudomonas aeruginosa* in an in vitro biofilm pharmacodynamic model. *Int. J. Antimicrob. Agents* **2019**, *53*, 612–619. [[CrossRef](#)]
21. Yang, Y.; Rasmussen, B.A.; Shlaes, D.M. Class A β -lactamases—Enzyme-inhibitor interactions and resistance. *Pharmacol. Therap.* **1999**, *83*, 141–151. [[CrossRef](#)] [[PubMed](#)]
22. Donnelley, M.A.; Zhu, E.S.; Thompson, G.R., 3rd. Isavuconazole in the treatment of invasive aspergillosis and mucormycosis infections. *Infect. Drug Resist.* **2016**, *9*, 79–86. [[PubMed](#)]
23. Ledoux, M.P.; Denis, J.; Nivoix, Y.; Herbrecht, R. Isavuconazole: A new broad-spectrum azole. Part 2: Pharmacokinetics and clinical activity. *J. Mycol. Med.* **2018**, *28*, 15–22. [[CrossRef](#)] [[PubMed](#)]
24. Taha, M.; Rahim, F.; Uddin, N.; Khan, I.U.; Iqbal, N.; Salauddin, M.; Farooq, R.K.; Gollapalli, M.; Khan, K.M.; Zafar, A. Exploring indole-based-thiadiazole derivatives as potent acetylcholinesterase and butyrylcholinesterase enzyme inhibitors. *Inter. J. Biol. Macromol.* **2021**, *188*, 1025–1036. [[CrossRef](#)]
25. Rahim, F.; Javid, M.T.; Ullah, H.; Wadood, A.; Taha, M.; Ashraf, M.; Aine, Q.U.; Khan, M.A.; Khan, F.; Mirza, S.; et al. Synthesis, Molecular Docking, Acetylcholinesterase and Butyrylcholinesterase Inhibitory Potential of Thiazole Analogs as New Inhibitors for Alzheimer Disease. *Bioorg. Chem.* **2015**, *62*, 106–116. [[CrossRef](#)]
26. Taha, M.; Alshamrani, F.J.; Rahim, F.; Uddin, N.; Chigurupati, S.; Almandil, N.B.; Farooq, R.K.; Iqbal, N.; Aldubayan, M.; Venugopal, V.; et al. Synthesis, characterization, biological evaluation, and kinetic study of indole base sulfonamide derivatives as acetylcholinesterase inhibitors in search of potent anti-Alzheimer agent. *J. King Saud Univ.-Sci.* **2021**, *33*, 101401. [[CrossRef](#)]
27. Taha, M.; Rahim, F.; Zaman, K.; Anouar, E.H.; Uddin, N.; Nawaz, F.; Sajid, M.; Khan, K.M.; Shah, A.A.; Wadood, A.; et al. Synthesis, in vitro biological screening and docking study of benzo [d] oxazole bis Schiff base derivatives as a potent anti-Alzheimer agent. *J. Biomole. Struct. Dyn.* **2021**, 1–16. [[CrossRef](#)]
28. Hussain, R.; Ullah, H.; Rahim, F.; Sarfraz, M.; Taha, M.; Iqbal, R.; Alhomrani, M.; Alamri, A.S.; Abdulaziz, O.; Abdelaziz, M.A. Multipotent Cholinesterase Inhibitors for the Treatment of Alzheimer's disease: Synthesis, Biological Analysis and Molecular Docking Study of Benzimidazole-Based Thiazole Derivatives. *Molecules* **2022**, *27*, 6087. [[CrossRef](#)]
29. Basha, N.M.; Venkatesh, B.C.; Reddy, G.M.; Zyryanov, G.V.; Subbaiah, M.V.; Wen, J.C.; Gollakota, A.R. Synthesis, Antimicrobial Assay and SARs of Pyrazole Included Heterocyclic Derivatives. *Polycycl. Aromat. Compd.* **2021**, 1–15. [[CrossRef](#)]
30. Shyamsivappan, S.; Vivek, R.; Saravanan, A.; Arasakumar, T.; Suresh, T.; Athimoolam, S.; Mohan, P.S. A novel 8-nitro quinoline-thiosemicarbazone analogues induces G1/S & G2/M phase cell cycle arrest and apoptosis through ROS mediated mitochondrial pathway. *Bioorganic Chem.* **2020**, *97*, 103709.
31. Riaz, N.; Iftikhar, M.; Saleem, M.; Hussain, S.; Rehmat, F.; Afzal, Z.; Khawar, S.; Ashraf, M.; al-Rashida, M. New synthetic 1,2,4-triazole derivatives: Cholinesterase inhibition and molecular docking studies. *Results Chem.* **2020**, *2*, 100041. [[CrossRef](#)]
32. Siddiqui, S.Z.; Arfan, M.; Abbasi, M.A.; Shah, S.A.A.; Ashraf, M.; Hussain, S.; Saleem, R.S.Z.; Rafique, R.; Khan, K.M. Discovery of Dual Inhibitors of Acetyl and Butyrylcholinesterase and Antiproliferative Activity of 1,2,4-Triazole-3-thiol: Synthesis and In Silico Molecular Study. *Chem. Select.* **2020**, *5*, 6430–6439. [[CrossRef](#)]
33. Wadood, A.; Shareef, A.; Rehman, A.U.; Muhammad, S.; Khurshid, B.; Khan, R.S.; Shams, S.; Afridi, S.G. In Silico Drug Designing for ala438 Deleted Ribosomal Protein S1 (RpsA) on the Basis of the Active Compound Zrl15. *ACS Omega* **2022**, *7*, 397–408. [[CrossRef](#)]
34. Rehman, A.U.; Zhen, G.; Zhong, B.; Ni, D.; Li, J.; Nasir, A.; Gabr, M.T.; Rafiq, H.; Wadood, A.; Lu, S.; et al. Mechanism of zinc ejection by disulfiram in nonstructural protein 5A. *Phys. Chem. Chem. Phys.* **2021**, *23*, 12204–12215. [[CrossRef](#)]
35. Chigurupati, S.; Selvaraj, M.; Mani, V.; Selvarajan, K.K.; Mohammad, J.I.; Kaveti, B.; Bera, H.; Palanimuthu, V.R.; Teh, L.K.; Salleh, M.Z. Identification of novel acetylcholinesterase inhibitors: Indolopyrazoline derivatives and molecular docking studies. *Bioorganic Chem.* **2016**, *67*, 9–17. [[CrossRef](#)]
36. Chigurupati, S.; Selvaraj, M.; Mani, V.; Mohammad, J.I.; Selvarajan, K.K.; Akhtar, S.S.; Marikannan, M.; Raj, S.; Teh, L.K.; Salleh, M.Z. Synthesis of azomethines derived from cinnamaldehyde and vanillin: In vitro acetylcholinesterase inhibitory, antioxidant and insilico molecular docking studies. *Med. Chem. Res.* **2018**, *27*, 807–816. [[CrossRef](#)]

Disclaimer/Publisher's Note: The statements, opinions and data contained in all publications are solely those of the individual author(s) and contributor(s) and not of MDPI and/or the editor(s). MDPI and/or the editor(s) disclaim responsibility for any injury to people or property resulting from any ideas, methods, instructions or products referred to in the content.